

Search for the Rare Decays $B^+ \rightarrow \mu^+ \mu^- K^+$, $B^0 \rightarrow \mu^+ \mu^- K^*(892)^0$, and $B_s^0 \rightarrow \mu^+ \mu^- \phi$ at CDF

T. Aaltonen,²⁴ J. Adelman,¹⁴ T. Akimoto,⁵⁶ M.G. Albrow,¹⁸ B. Álvarez González,¹² S. Amerio^u,⁴⁴ D. Amidei,³⁵ A. Anastassov,³⁹ A. Annovi,²⁰ J. Antos,¹⁵ G. Apollinari,¹⁸ A. Apresyan,⁴⁹ T. Arisawa,⁵⁸ A. Artikov,¹⁶ W. Ashmanskas,¹⁸ A. Attal,⁴ A. Aurisano,⁵⁴ F. Azfar,⁴³ P. Azzurri^s,⁴⁷ W. Badgett,¹⁸ A. Barbaro-Galtieri,²⁹ V.E. Barnes,⁴⁹ B.A. Barnett,²⁶ V. Bartsch,³¹ G. Bauer,³³ P.-H. Beauchemin,³⁴ F. Bedeschi,⁴⁷ P. Bednar,¹⁵ D. Beecher,³¹ S. Behari,²⁶ G. Bellettini^q,⁴⁷ J. Bellinger,⁶⁰ D. Benjamin,¹⁷ A. Beretvas,¹⁸ J. Beringer,²⁹ A. Bhatti,⁵¹ M. Binkley,¹⁸ D. Bisello^u,⁴⁴ I. Bizjak,³¹ R.E. Blair,² C. Blocker,⁷ B. Blumenfeld,²⁶ A. Bocci,¹⁷ A. Bodek,⁵⁰ V. Boisvert,⁵⁰ G. Bolla,⁴⁹ D. Bortoletto,⁴⁹ J. Boudreau,⁴⁸ A. Boveia,¹¹ B. Brau,¹¹ A. Bridgeman,²⁵ L. Brigliadori,⁴⁴ C. Bromberg,³⁶ E. Brubaker,¹⁴ J. Budagov,¹⁶ H.S. Budd,⁵⁰ S. Budd,²⁵ K. Burkett,¹⁸ G. Busetto^u,⁴⁴ P. Bussey^x,²² A. Buzatu,³⁴ K. L. Byrum,² S. Cabrera^p,¹⁷ C. Calancha,³² M. Campanelli,³⁶ M. Campbell,³⁵ F. Canelli,¹⁸ A. Canepa,⁴⁶ D. Carlsmith,⁶⁰ R. Carosi,⁴⁷ S. Carrillo^j,¹⁹ S. Carron,³⁴ B. Casal,¹² M. Casarsa,¹⁸ A. Castro^t,⁶ P. Catastini^r,⁴⁷ D. Cauz^w,⁵⁵ V. Cavaliere^r,⁴⁷ M. Cavalli-Sforza,⁴ A. Cerri,²⁹ L. Cerritoⁿ,³¹ S.H. Chang,²⁸ Y.C. Chen,¹ M. Chertok,⁸ G. Chiarelli,⁴⁷ G. Chlachidze,¹⁸ F. Chlebana,¹⁸ K. Cho,²⁸ D. Chokheli,¹⁶ J.P. Chou,²³ G. Choudalakis,³³ S.H. Chuang,⁵³ K. Chung,¹³ W.H. Chung,⁶⁰ Y.S. Chung,⁵⁰ C.I. Ciobanu,⁴⁵ M.A. Ciocci^r,⁴⁷ A. Clark,²¹ D. Clark,⁷ G. Compostella,⁴⁴ M.E. Convery,¹⁸ J. Conway,⁸ K. Copic,³⁵ M. Cordelli,²⁰ G. Cortiana^u,⁴⁴ D.J. Cox,⁸ F. Crescioli^q,⁴⁷ C. Cuenca Almenar^p,⁸ J. Cuevas^m,¹² R. Culbertson,¹⁸ J.C. Cully,³⁵ D. Dagenhart,¹⁸ M. Datta,¹⁸ T. Davies,²² P. de Barbaro,⁵⁰ S. De Cecco,⁵² A. Deisher,²⁹ G. De Lorenzo,⁴ M. Dell'Orso^q,⁴⁷ C. Deluca,⁴ L. Demortier,⁵¹ J. Deng,¹⁷ M. Deninno,⁶ P.F. Derwent,¹⁸ G.P. di Giovanni,⁴⁵ C. Dionisi^v,⁵² B. Di Ruzza^w,⁵⁵ J.R. Dittmann,⁵ M. D'Onofrio,⁴ S. Donati^q,⁴⁷ P. Dong,⁹ J. Donini,⁴⁴ T. Dorigo,⁴⁴ S. Dube,⁵³ J. Efron,⁴⁰ A. Elagin,⁵⁴ R. Erbacher,⁸ D. Errede,²⁵ S. Errede,²⁵ R. Eusebi,¹⁸ H.C. Fang,²⁹ S. Farrington,⁴³ W.T. Fedorko,¹⁴ R.G. Feild,⁶¹ M. Feindt,²⁷ J.P. Fernandez,³² C. Ferrazza^s,⁴⁷ R. Field,¹⁹ G. Flanagan,⁴⁹ R. Forrest,⁸ M. Franklin,²³ J.C. Freeman,¹⁸ I. Furic,¹⁹ M. Gallinaro,⁵² J. Galyardt,¹³ F. Garbersen,¹¹ J.E. Garcia,⁴⁷ A.F. Garfinkel,⁴⁹ K. Genser,¹⁸ H. Gerberich,²⁵ D. Gerdes,³⁵ A. Gessler,²⁷ S. Giagu^v,⁵² V. Giakoumopoulou,³ P. Giannetti,⁴⁷ K. Gibson,⁴⁸ J.L. Gimmell,⁵⁰ C.M. Ginsburg,¹⁸ N. Giokaris,³ M. Giordani^w,⁵⁵ P. Giromini,²⁰ M. Giunta^q,⁴⁷ G. Giurgiu,²⁶ V. Glagolev,¹⁶ D. Glenzinski,¹⁸ M. Gold,³⁸ N. Goldschmidt,¹⁹ A. Golossanov,¹⁸ G. Gomez,¹² G. Gomez-Ceballos,³³ M. Goncharov,⁵⁴ O. González,³² I. Gorelov,³⁸ A.T. Goshaw,¹⁷ K. Goulianos,⁵¹ A. Gresele^u,⁴⁴ S. Grinstein,²³ C. Grosso-Pilcher,¹⁴ R.C. Group,¹⁸ U. Grundler,²⁵ J. Guimaraes da Costa,²³ Z. Gunay-Unalan,³⁶ C. Haber,²⁹ K. Hahn,³³ S.R. Hahn,¹⁸ E. Halkiadakis,⁵³ B.-Y. Han,⁵⁰ J.Y. Han,⁵⁰ R. Handler,⁶⁰ F. Happacher,²⁰ K. Hara,⁵⁶ D. Hare,⁵³ M. Hare,⁵⁷ S. Harper,⁴³ R.F. Harr,⁵⁹ R.M. Harris,¹⁸ M. Hartz,⁴⁸ K. Hatakeyama,⁵¹ J. Hauser,⁹ C. Hays,⁴³ M. Heck,²⁷ A. Heijboer,⁴⁶ B. Heinemann,²⁹ J. Heinrich,⁴⁶ C. Henderson,³³ M. Herndon,⁶⁰ J. Heuser,²⁷ S. Hewamanage,⁵ D. Hidas,¹⁷ C.S. Hill^c,¹¹ D. Hirschbuehl,²⁷ A. Hocker,¹⁸ S. Hou,¹ M. Houlden,³⁰ S.-C. Hsu,¹⁰ B.T. Huffman,⁴³ R.E. Hughes,⁴⁰ U. Husemann,⁶¹ J. Huston,³⁶ J. Incandela,¹¹ G. Introzzi,⁴⁷ M. Iori^v,⁵² A. Ivanov,⁸ E. James,¹⁸ B. Jayatilaka,¹⁷ E.J. Jeon,²⁸ M.K. Jha,⁶ S. Jindariani,¹⁸ W. Johnson,⁸ M. Jones,⁴⁹ K.K. Joo,²⁸ S.Y. Jun,¹³ J.E. Jung,²⁸ T.R. Junk,¹⁸ T. Kamon,⁵⁴ D. Kar,¹⁹ P.E. Karchin,⁵⁹ Y. Kato,⁴² R. Kephart,¹⁸ J. Keung,⁴⁶ V. Khotilovich,⁵⁴ B. Kilminster,⁴⁰ D.H. Kim,²⁸ H.S. Kim,²⁸ J.E. Kim,²⁸ M.J. Kim,²⁰ S.B. Kim,²⁸ S.H. Kim,⁵⁶ Y.K. Kim,¹⁴ N. Kimura,⁵⁶ L. Kirsch,⁷ S. Klimentenko,¹⁹ B. Knuteson,³³ B.R. Ko,¹⁷ S.A. Koay,¹¹ K. Kondo,⁵⁸ D.J. Kong,²⁸ J. Konigsberg,¹⁹ A. Korytov,¹⁹ A.V. Kotwal,¹⁷ M. Kreps,²⁷ J. Kroll,⁴⁶ N. Krumnack,⁵ M. Kruse,¹⁷ V. Krutelyov,¹¹ T. Kubo,⁵⁶ T. Kuhr,²⁷ N.P. Kulkarni,⁵⁹ M. Kurata,⁵⁶ Y. Kusakabe,⁵⁸ S. Kwang,¹⁴ A.T. Laasanen,⁴⁹ S. Lami,⁴⁷ S. Lammel,¹⁸ M. Lancaster,³¹ R.L. Lander,⁸ K. Lannon,⁴⁰ A. Lath,⁵³ G. Latino^r,⁴⁷ I. Lazzizzera^u,⁴⁴ T. LeCompte,² E. Lee,⁵⁴ S.W. Lee^o,⁵⁴ S. Leone,⁴⁷ S. Levy,¹⁴ J.D. Lewis,¹⁸ C.S. Lin,²⁹ J. Linacre,⁴³ M. Lindgren,¹⁸ E. Lipeles,¹⁰ A. Lister,⁸ D.O. Litvintsev,¹⁸ C. Liu,⁴⁸ T. Liu,¹⁸ N.S. Lockyer,⁴⁶ A. Loginov,⁶¹ M. Loretini^u,⁴⁴ L. Lovas,¹⁵ R.-S. Lu,¹ D. Lucchesi^u,⁴⁴ J. Lueck,²⁷ C. Luci^v,⁵² P. Lujan,²⁹ P. Lukens,¹⁸ G. Lungu,⁵¹ L. Lyons,⁴³ J. Lys,²⁹ R. Lysak,¹⁵ E. Lytken,⁴⁹ P. Mack,²⁷ D. MacQueen,³⁴ R. Madrak,¹⁸ K. Maeshima,¹⁸ K. Makhoul,³³ T. Maki,²⁴ P. Maksimovic,²⁶ S. Malde,⁴³ S. Malik,³¹ G. Manca,³⁰ A. Manousakis-Katsikakis,³ F. Margaroli,⁴⁹ C. Marino,²⁷ C.P. Marino,²⁵ A. Martin,⁶¹ V. Martinⁱ,²² M. Martínez,⁴ R. Martínez-Ballarín,³² T. Maruyama,⁵⁶ P. Mastrandrea,⁵² T. Masubuchi,⁵⁶ M.E. Mattson,⁵⁹ P. Mazzanti,⁶ K.S. McFarland,⁵⁰ P. McIntyre,⁵⁴ R. McNulty^h,³⁰ A. Mehta,³⁰ P. Mehtala,²⁴ A. Menzione,⁴⁷ P. Merkel,⁴⁹ C. Mesropian,⁵¹ T. Miao,¹⁸ N. Miladinovic,⁷ R. Miller,³⁶ C. Mills,²³ M. Milnik,²⁷ A. Mitra,¹ G. Mitselmakher,¹⁹ H. Miyake,⁵⁶ N. Moggi,⁶ C.S. Moon,²⁸ R. Moore,¹⁸ M.J. Morello^q,⁴⁷ J. Morlok,²⁷ P. Movilla Fernandez,¹⁸ J. Mülmenstädt,²⁹ A. Mukherjee,¹⁸ Th. Muller,²⁷ R. Mumford,²⁶ P. Murat,¹⁸ M. Mussini^t,⁶ J. Nachtman,¹⁸ Y. Nagai,⁵⁶ A. Nagano,⁵⁶ J. Naganoma,⁵⁸ K. Nakamura,⁵⁶ I. Nakano,⁴¹ A. Napier,⁵⁷ V. Necula,¹⁷ C. Neu,⁴⁶

M.S. Neubauer,²⁵ J. Nielsen^e,²⁹ L. Nodulman,² M. Norman,¹⁰ O. Norniella,²⁵ E. Nurse,³¹ L. Oakes,⁴³ S.H. Oh,¹⁷ Y.D. Oh,²⁸ I. Oksuzian,¹⁹ T. Okusawa,⁴² R. Oldeman,³⁰ R. Orava,²⁴ K. Osterberg,²⁴ S. Pagan Griso^u,⁴⁴ C. Pagliarone,⁴⁷ E. Palencia,¹⁸ V. Papadimitriou,¹⁸ A. Papaikononou,²⁷ A.A. Paramonov,¹⁴ B. Parks,⁴⁰ S. Pashapour,³⁴ J. Patrick,¹⁸ G. Pauletta^w,⁵⁵ M. Paulini,¹³ C. Paus,³³ D.E. Pellett,⁸ A. Penzo,⁵⁵ T.J. Phillips,¹⁷ G. Piacentino,⁴⁷ E. Pianori,⁴⁶ L. Pinera,¹⁹ K. Pitts,²⁵ C. Plager,⁹ L. Pondrom,⁶⁰ O. Poukhov,¹⁶ N. Pounder,⁴³ F. Prakoshyn,¹⁶ A. Pronko,¹⁸ J. Proudfoot,² F. Ptohos^g,¹⁸ E. Pueschel,¹³ G. Punzi^q,⁴⁷ J. Pursley,⁶⁰ J. Rademacker^c,⁴³ A. Rahaman,⁴⁸ V. Ramakrishnan,⁶⁰ N. Ranjan,⁴⁹ I. Redondo,³² B. Reiser,¹⁸ V. Rekovic,³⁸ P. Renton,⁴³ M. Rescigno,⁵² S. Richter,²⁷ F. Rimondi^t,⁶ L. Ristori,⁴⁷ A. Robson,²² T. Rodrigo,¹² T. Rodriguez,⁴⁶ E. Rogers,²⁵ S. Rolli,⁵⁷ R. Roser,¹⁸ M. Rossi,⁵⁵ R. Rossin,¹¹ P. Roy,³⁴ A. Ruiz,¹² J. Russ,¹³ V. Rusu,¹⁸ H. Saarikko,²⁴ A. Safonov,⁵⁴ W.K. Sakumoto,⁵⁰ O. Saltó,⁴ L. Santi^w,⁵⁵ S. Sarkar^v,⁵² L. Sartori,⁴⁷ K. Sato,¹⁸ A. Savoy-Navarro,⁴⁵ T. Scheidle,²⁷ P. Schlabach,¹⁸ A. Schmidt,²⁷ E.E. Schmidt,¹⁸ M.A. Schmidt,¹⁴ M.P. Schmidt^{*},⁶¹ M. Schmitt,³⁹ T. Schwarz,⁸ L. Scodellaro,¹² A.L. Scott,¹¹ A. Scribano^r,⁴⁷ F. Scuri,⁴⁷ A. Sedov,⁴⁹ S. Seidel,³⁸ Y. Seiya,⁴² A. Semenov,¹⁶ L. Sexton-Kennedy,¹⁸ A. Sfyrla,²¹ S.Z. Shalhout,⁵⁹ T. Shears,³⁰ P.F. Shepard,⁴⁸ D. Sherman,²³ M. Shimojima^l,⁵⁶ S. Shiraishi,¹⁴ M. Shochet,¹⁴ Y. Shon,⁶⁰ I. Shreyber,³⁷ A. Sidoti,⁴⁷ P. Sinervo,³⁴ A. Sisakyan,¹⁶ A.J. Slaughter,¹⁸ J. Slaunwhite,⁴⁰ K. Sliwa,⁵⁷ J.R. Smith,⁸ F.D. Snider,¹⁸ R. Snihur,³⁴ A. Soha,⁸ S. Somalwar,⁵³ V. Sorin,³⁶ J. Spalding,¹⁸ T. Spreitzer,³⁴ P. Squillacioti^r,⁴⁷ M. Stanitzki,⁶¹ R. St. Denis,²² B. Stelzer,⁹ O. Stelzer-Chilton,⁴³ D. Stentz,³⁹ J. Strologas,³⁸ D. Stuart,¹¹ J.S. Suh,²⁸ A. Sukhanov,¹⁹ I. Suslov,¹⁶ T. Suzuki,⁵⁶ A. Taffard^d,²⁵ R. Takashima,⁴¹ Y. Takeuchi,⁵⁶ R. Tanaka,⁴¹ M. Tecchio,³⁵ P.K. Teng,¹ K. Terashi,⁵¹ R.J. Tesarek,¹⁸ J. Thom^f,¹⁸ A.S. Thompson,²² G.A. Thompson,²⁵ E. Thomson,⁴⁶ P. Tipton,⁶¹ V. Tiwari,¹³ S. Tkaczyk,¹⁸ D. Toback,⁵⁴ S. Tokar,¹⁵ K. Tollefson,³⁶ T. Tomura,⁵⁶ D. Tonelli,¹⁸ S. Torre,²⁰ D. Torretta,¹⁸ P. Totaro^w,⁵⁵ S. Tourneur,⁴⁵ Y. Tu,⁴⁶ N. Turini^r,⁴⁷ F. Ukegawa,⁵⁶ S. Vallecorsa,²¹ N. van Remortel^a,²⁴ A. Varganov,³⁵ E. Vataga^s,⁴⁷ F. Vázquez^j,¹⁹ G. Velev,¹⁸ C. Vellidis,³ V. Veszpremi,⁴⁹ M. Vidal,³² R. Vidal,¹⁸ I. Vila,¹² R. Vilar,¹² T. Vine,³¹ M. Vogel,³⁸ I. Volobouev^o,²⁹ G. Volpi^q,⁴⁷ F. Würthwein,¹⁰ P. Wagner,² R.G. Wagner,² R.L. Wagner,¹⁸ J. Wagner-Kuhr,²⁷ W. Wagner,²⁷ T. Wakisaka,⁴² R. Wallny,⁹ S.M. Wang,¹ A. Warburton,³⁴ D. Waters,³¹ M. Weinberger,⁵⁴ W.C. Wester III,¹⁸ B. Whitehouse,⁵⁷ D. Whiteson^d,⁴⁶ A.B. Wicklund,² E. Wicklund,¹⁸ G. Williams,³⁴ H.H. Williams,⁴⁶ P. Wilson,¹⁸ B.L. Winer,⁴⁰ P. Wittich^f,¹⁸ S. Wolbers,¹⁸ C. Wolfe,¹⁴ T. Wright,³⁵ X. Wu,²¹ S.M. Wynne,³⁰ A. Yagil,¹⁰ K. Yamamoto,⁴² J. Yamaoka,⁵³ U.K. Yang^k,¹⁴ Y.C. Yang,²⁸ W.M. Yao,²⁹ G.P. Yeh,¹⁸ J. Yoh,¹⁸ K. Yorita,¹⁴ T. Yoshida,⁴² G.B. Yu,⁵⁰ I. Yu,²⁸ S.S. Yu,¹⁸ J.C. Yun,¹⁸ L. Zanello^v,⁵² A. Zanetti,⁵⁵ I. Zaw,²³ X. Zhang,²⁵ Y. Zheng^b,⁹ and S. Zucchelli^{t6}

(CDF Collaboration[†])

¹*Institute of Physics, Academia Sinica, Taipei, Taiwan 11529, Republic of China*

²*Argonne National Laboratory, Argonne, Illinois 60439*

³*University of Athens, 157 71 Athens, Greece*

⁴*Institut de Fisica d'Altes Energies, Universitat Autònoma de Barcelona, E-08193, Bellaterra (Barcelona), Spain*

⁵*Baylor University, Waco, Texas 76798*

⁶*Istituto Nazionale di Fisica Nucleare Bologna, ⁴University of Bologna, I-40127 Bologna, Italy*

⁷*Brandeis University, Waltham, Massachusetts 02254*

⁸*University of California, Davis, Davis, California 95616*

⁹*University of California, Los Angeles, Los Angeles, California 90024*

¹⁰*University of California, San Diego, La Jolla, California 92093*

¹¹*University of California, Santa Barbara, Santa Barbara, California 93106*

¹²*Instituto de Fisica de Cantabria, CSIC-University of Cantabria, 39005 Santander, Spain*

¹³*Carnegie Mellon University, Pittsburgh, PA 15213*

¹⁴*Enrico Fermi Institute, University of Chicago, Chicago, Illinois 60637*

¹⁵*Comenius University, 842 48 Bratislava, Slovakia; Institute of Experimental Physics, 040 01 Kosice, Slovakia*

¹⁶*Joint Institute for Nuclear Research, RU-141980 Dubna, Russia*

¹⁷*Duke University, Durham, North Carolina 27708*

¹⁸*Fermi National Accelerator Laboratory, Batavia, Illinois 60510*

¹⁹*University of Florida, Gainesville, Florida 32611*

²⁰*Laboratori Nazionali di Frascati, Istituto Nazionale di Fisica Nucleare, I-00044 Frascati, Italy*

²¹*University of Geneva, CH-1211 Geneva 4, Switzerland*

²²*Glasgow University, Glasgow G12 8QQ, United Kingdom*

²³*Harvard University, Cambridge, Massachusetts 02138*

²⁴*Division of High Energy Physics, Department of Physics,*

University of Helsinki and Helsinki Institute of Physics, FIN-00014, Helsinki, Finland

²⁵*University of Illinois, Urbana, Illinois 61801*

²⁶*The Johns Hopkins University, Baltimore, Maryland 21218*

²⁷*Institut für Experimentelle Kernphysik, Universität Karlsruhe, 76128 Karlsruhe, Germany*

- ²⁸Center for High Energy Physics: Kyungpook National University, Daegu 702-701, Korea; Seoul National University, Seoul 151-742, Korea; Sungkyunkwan University, Suwon 440-746, Korea; Korea Institute of Science and Technology Information, Daejeon, 305-806, Korea; Chonnam National University, Gwangju, 500-757, Korea
- ²⁹Ernest Orlando Lawrence Berkeley National Laboratory, Berkeley, California 94720
- ³⁰University of Liverpool, Liverpool L69 7ZE, United Kingdom
- ³¹University College London, London WC1E 6BT, United Kingdom
- ³²Centro de Investigaciones Energeticas Medioambientales y Tecnologicas, E-28040 Madrid, Spain
- ³³Massachusetts Institute of Technology, Cambridge, Massachusetts 02139
- ³⁴Institute of Particle Physics: McGill University, Montréal, Canada H3A 2T8; and University of Toronto, Toronto, Canada M5S 1A7
- ³⁵University of Michigan, Ann Arbor, Michigan 48109
- ³⁶Michigan State University, East Lansing, Michigan 48824
- ³⁷Institution for Theoretical and Experimental Physics, ITEP, Moscow 117259, Russia
- ³⁸University of New Mexico, Albuquerque, New Mexico 87131
- ³⁹Northwestern University, Evanston, Illinois 60208
- ⁴⁰The Ohio State University, Columbus, Ohio 43210
- ⁴¹Okayama University, Okayama 700-8530, Japan
- ⁴²Osaka City University, Osaka 588, Japan
- ⁴³University of Oxford, Oxford OX1 3RH, United Kingdom
- ⁴⁴Istituto Nazionale di Fisica Nucleare, Sezione di Padova-Trento, ^uUniversity of Padova, I-35131 Padova, Italy
- ⁴⁵LPNHE, Universite Pierre et Marie Curie/IN2P3-CNRS, UMR7585, Paris, F-75252 France
- ⁴⁶University of Pennsylvania, Philadelphia, Pennsylvania 19104
- ⁴⁷Istituto Nazionale di Fisica Nucleare Pisa, ^qUniversity of Pisa, ^rUniversity of Siena and ^sScuola Normale Superiore, I-56127 Pisa, Italy
- ⁴⁸University of Pittsburgh, Pittsburgh, Pennsylvania 15260
- ⁴⁹Purdue University, West Lafayette, Indiana 47907
- ⁵⁰University of Rochester, Rochester, New York 14627
- ⁵¹The Rockefeller University, New York, New York 10021
- ⁵²Istituto Nazionale di Fisica Nucleare, Sezione di Roma 1, ^vSapienza Università di Roma, I-00185 Roma, Italy
- ⁵³Rutgers University, Piscataway, New Jersey 08855
- ⁵⁴Texas A&M University, College Station, Texas 77843
- ⁵⁵Istituto Nazionale di Fisica Nucleare Trieste/ Udine, ^wUniversity of Trieste/ Udine, Italy
- ⁵⁶University of Tsukuba, Tsukuba, Ibaraki 305, Japan
- ⁵⁷Tufts University, Medford, Massachusetts 02155
- ⁵⁸Waseda University, Tokyo 169, Japan
- ⁵⁹Wayne State University, Detroit, Michigan 48201
- ⁶⁰University of Wisconsin, Madison, Wisconsin 53706
- ⁶¹Yale University, New Haven, Connecticut 06520

We search for $b \rightarrow s\mu^+\mu^-$ transitions in B meson (B^+ , B^0 , or B_s^0) decays with 924 pb^{-1} of $p\bar{p}$ collisions at $\sqrt{s} = 1.96\text{ TeV}$ collected with the CDF II detector at the Fermilab Tevatron. We find excesses with significances of 4.5, 2.9, and 2.4 standard deviations in the $B^+ \rightarrow \mu^+\mu^-K^+$, $B^0 \rightarrow \mu^+\mu^-K^*(892)^0$, and $B_s^0 \rightarrow \mu^+\mu^-\phi$ decay modes, respectively. Using $B \rightarrow J/\psi h$ ($h = K^+$, $K^*(892)^0$, ϕ) decays as normalization channels, we report branching fractions for the previously observed B^+ and B^0 decays, $\mathcal{B}(B^+ \rightarrow \mu^+\mu^-K^+) = (0.59 \pm 0.15 \pm 0.04) \times 10^{-6}$, and $\mathcal{B}(B^0 \rightarrow \mu^+\mu^-K^*(892)^0) = (0.81 \pm 0.30 \pm 0.10) \times 10^{-6}$, where the first uncertainty is statistical, and the second is systematic. These measurements are consistent with the world average results, and are competitive with the best available measurements. We set an upper limit on the relative branching fraction $\frac{\mathcal{B}(B_s^0 \rightarrow \mu^+\mu^-\phi)}{\mathcal{B}(B_s^0 \rightarrow J/\psi\phi)} < 2.6(2.3) \times 10^{-3}$ at the 95(90)% confidence level, which is the most stringent to date.

PACS numbers: Valid PACS appear here

*Deceased

[†]With visitors from ^aUniversiteit Antwerpen, B-2610 Antwerp, Belgium, ^bChinese Academy of Sciences, Beijing 100864, China, ^cUniversity of Bristol, Bristol BS8 1TL, United Kingdom,

^dUniversity of California Irvine, Irvine, CA 92697, ^eUniversity of California Santa Cruz, Santa Cruz, CA 95064, ^fCornell University, Ithaca, NY 14853, ^gUniversity of Cyprus, Nicosia CY-1678,

The decay of a b quark into an s quark and two muons ($b \rightarrow s\mu^+\mu^-$) is a flavor-changing neutral current process, forbidden at tree level in the standard model (SM) but allowed through highly suppressed internal loops. New physics could manifest itself in a larger branching fraction, a modified dimuon mass distribution, or angular distributions of the decay products different from that predicted by the SM [1, 2, 3, 4]. In this paper, we report branching ratio measurements of exclusive decays, where the s quark hadronizes into a single meson. Reconstructing a final state with only three or four charged final state particles results in smaller backgrounds than those expected in a search for inclusive $B \rightarrow X_s\mu^+\mu^-$ decays. The rare decays, $B^+ \rightarrow \mu^+\mu^-K^+$ and $B^0 \rightarrow \mu^+\mu^-K^*(892)^0$ have been observed at the B factories [5, 6], with branching fractions of $O(10^{-6})$, consistent with SM predictions [7, 8, 9, 10, 11, 12, 13, 14]. The analogous decay in the B_s system, $B_s^0 \rightarrow \mu^+\mu^-\phi$, has a predicted branching ratio of 1.6×10^{-6} [15], but has not yet been observed [16, 17]. We report branching ratio measurements from 924 pb $^{-1}$ of Collider Detector at Fermilab (CDF) Run II data that pave the way for future studies of larger datasets from which kinematic distributions may be measured. We search for $B \rightarrow \mu^+\mu^-h$ decays, where B stands for B^+ , B^0 , or B_s^0 , and h stands for K^+ , $K^*(892)^0$, or ϕ , respectively. The $K^*(892)^0$, referred to as K^{*0} throughout this paper, is reconstructed in the $K^{*0} \rightarrow K^+\pi^-$, decay mode, and the ϕ meson is reconstructed as $\phi \rightarrow K^+K^-$. We measure branching ratios relative to $B \rightarrow J/\psi h$ decays, followed by $J/\psi \rightarrow \mu^+\mu^-$ decays, resulting in the same final state particles as the rare decay modes. Many systematic uncertainties cancel in the relative branching ratios:

$$\frac{\mathcal{B}(B \rightarrow \mu^+\mu^-h)}{\mathcal{B}(B \rightarrow J/\psi h)} = \frac{N_{\mu^+\mu^-h}}{N_{J/\psi h}} \frac{\epsilon_{J/\psi h}}{\epsilon_{\mu^+\mu^-h}} \times \mathcal{B}(J/\psi \rightarrow \mu^+\mu^-), \quad (1)$$

where $N_{\mu^+\mu^-h}$ is the observed number of $B \rightarrow \mu^+\mu^-h$ decays, $N_{J/\psi h}$ is the observed number of $B \rightarrow J/\psi h$ decays, while $\epsilon_{J/\psi h}$ and $\epsilon_{\mu^+\mu^-h}$ are the combined selection efficiency and acceptance of the experiment for $B \rightarrow J/\psi h$ and $B \rightarrow \mu^+\mu^-h$ respectively. Throughout this report, charge conjugate modes are implicitly included.

CDF II is a general purpose detector, located at the Tevatron $p\bar{p}$ collider [18]. Charged particle trajectories (tracks) are detected by the tracking system comprised of a seven-layer double-sided silicon microstrip detector and

a drift chamber, both in a 1.4 T axial magnetic field. The silicon detector [19] ranges in radius from 1.3 to 28 cm, and has a single-hit resolution of approximately 15 μm . The drift chamber [20] provides up to 96 measurements from radii of 40 to 137 cm with a single-hit resolution of approximately 180 μm . A muon chamber identification system of plastic scintillators and drift chambers [21] is located on the exterior of the detector with a central part covering $|\eta| < 0.6$, and an extended region covering $0.6 < |\eta| < 1.0$, where η is the pseudorapidity [22]. In the central(extended) region, muons are detected if their transverse momentum component, p_T , is greater than 1.5(2.0) GeV/ c . Events are selected with a three-level trigger system. The first trigger level requires the presence of two charged particles with $p_T \geq 1.5$ GeV/ c ($|\eta| \leq 0.6$) or $p_T \geq 2.0$ GeV/ c ($0.6 \leq |\eta| \leq 1.0$), matched to track segments in the muon chambers to form muon candidates. At the second level, a more restrictive selection is made by requiring that the muon candidates have opposite charge, and that their opening angle in the plane transverse to the beamline is less than 120°. At the third trigger level, the event is fully reconstructed. The trajectories of the muon candidates in the silicon detector are required to intersect at a point which is displaced transversely from the beamline by at least 100 μm .

The offline selection begins with a suppression of random combinations of tracks satisfying the selection requirements (combinatoric background), by requiring that all tracks have $p_T > 0.4$ GeV/ c and match hits from at least three layers of the silicon detector. The trajectories of a pair of muon candidates that satisfy the trigger requirements, and the tracks that form the hadron candidate, are fitted with the constraint that they originate from a single vertex in 3-dimensional space to form a B candidate. The χ^2 probability of the fit is required to be greater than 10^{-3} . A K^+ candidate is a track assigned the charged kaon mass, and the K^{*0} (ϕ) candidates are formed from oppositely charged pairs of tracks whose invariant mass must lie within 50 (10) MeV/ c^2 of the K^{*0} (ϕ) mass. For all particles, we use the world average values tabulated in Ref. [23]. The ambiguity of the mass assignment in $B^0 \rightarrow \mu^+\mu^-K^{*0}$ decays is handled by choosing the combination whose $K^+\pi^-$ mass is closer to the K^{*0} mass. In reconstructing the B candidates, the meson containing a strange quark, h , is required to have $p_T(h) \geq 1.0$ GeV/ c , and the B candidate is required to have $p_T(B) \geq 4.0$ GeV/ c . We require that the distance of closest approach between the flight path of the B candidate and the beamline, $|d_0(B)|$, is less than 120 μm , to reduce the combinatoric background with no loss of signal.

Normalization mode candidates are identified by having a dimuon invariant mass within 50 MeV/ c^2 of the J/ψ mass, yielding approximately 12 000 $B^+ \rightarrow J/\psi K^+$, 4400 $B^0 \rightarrow J/\psi K^{*0}$, and 800 $B_s^0 \rightarrow J/\psi \phi$ decays. The B candidate mass distributions of all modes are compatible with a Gaussian of width $\sigma = 20$ MeV/ c^2 . To reduce backgrounds from B decays to mesons contain-

Cyprus, ^hUniversity College Dublin, Dublin 4, Ireland, ⁱUniversity of Edinburgh, Edinburgh EH9 3JZ, United Kingdom, ^jUniversidad Iberoamericana, Mexico D.F., Mexico, ^kUniversity of Manchester, Manchester M13 9PL, England, ^lNagasaki Institute of Applied Science, Nagasaki, Japan, ^mUniversity de Oviedo, E-33007 Oviedo, Spain, ⁿQueen Mary, University of London, London, E1 4NS, England, ^oTexas Tech University, Lubbock, TX 79409, ^pIFIC(CSIC-Universitat de Valencia), 46071 Valencia, Spain, ^qRoyal Society of Edinburgh/Scottish Executive Support Research Fellow,

ing c quarks, several vetoes are applied to $B \rightarrow \mu^+ \mu^- h$ candidates, listed below. We eliminate candidates with a dimuon mass near the $J/\psi^{(\prime)}$: $2.9 \leq m_{\mu\mu} \leq 3.2 \text{ GeV}/c^2$ or $3.6 \leq m_{\mu\mu} \leq 3.75 \text{ GeV}/c^2$ respectively. $B \rightarrow J/\psi^{(\prime)} h$ decays followed by the radiative decay of the $J/\psi^{(\prime)}$ into two muons and a photon that is not reconstructed, may have a dimuon mass that passes the $J/\psi^{(\prime)}$ veto. We reject these events making use of the correlation between the candidate's invariant mass and the dimuon invariant mass, and require $|(m_{\mu\mu h} - m_B) - (m_{\mu\mu} - m_{J/\psi^{(\prime)}})| > 100 \text{ MeV}/c^2$. $B \rightarrow J/\psi^{(\prime)} h$ decays with one hadron misidentified as a muon form a potential background to the rare decay search. We reject this class of background by requiring that all combinations of tracks of the candidate have an invariant mass that differs by at least $40 \text{ MeV}/c^2$ from the $J/\psi^{(\prime)}$ mass. We also reject candidates with track pairs with a mass within $\pm 25 \text{ MeV}/c^2$ of the $D^0 \rightarrow K^- \pi^+$ decay, or track triplets compatible with a mass within $\pm 25 \text{ MeV}/c^2$ of the $D^+ \rightarrow K^- \pi^+ \pi^+$ or $D_s^+ \rightarrow K^+ K^- \pi^+$ decays.

We further improve the signal to background ratio by an optimization of the selection based on discriminating variables. For this purpose, Monte Carlo (MC) simulations of the signal processes are used. We generate single b hadrons using the transverse momentum spectrum from $B \rightarrow J/\psi X$, measured by CDF [18]. Decays of all b hadrons are simulated using EVTGEN [24], with lifetimes from Ref. [23], allowing for a decay width difference between the B_s^0 mass eigenstates, $\Delta\Gamma/\Gamma = 0.12 \pm 0.06$ [25]. The decays $B^0 \rightarrow J/\psi K^{*0}$ and $B_s^0 \rightarrow J/\psi \phi$ are simulated according to the polarization amplitudes measured by CDF [26]. The dynamics of the rare decay processes are simulated according to the calculations of Ali *et al.* [11]. For $B_s^0 \rightarrow \mu^+ \mu^- \phi$, we assume a mixture of 50% CP-even and 50% CP-odd states. The interactions of final state particles are simulated using a GEANT [27] model of the CDF II detector, digitized into the CDF event format, and reconstructed using the same software as in the processing of collision data. The detector simulation includes a full emulation of the CDF trigger system. We find that the transverse momentum spectrum of the B mesons of this measurement are on average higher than in the simulation. This can be explained by the presence of a B baryon component with low transverse momentum in the measurement used as input spectrum of the simulation [18]. To correct for this, the simulated events are weighted by a polynomial function, which is obtained from the ratio of data to MC transverse momentum distribution of the B meson.

We tighten the candidate selection to obtain the smallest expected statistical uncertainty on the measurement of the $B \rightarrow \mu^+ \mu^- h$ branching ratios by finding the selection with the largest value of $N_{sig}/\sqrt{N_{sig} + N_{bkg}}$. The expected number of signal events, N_{sig} , is determined by scaling the MC yields of the rare decay modes to the yields of the normalization channels in the data, and correcting by the relative branching ratios and selection efficiencies. This procedure requires estimates of

the branching ratios of the rare decay modes. For the $B^+ \rightarrow \mu^+ \mu^- K^+$ and $B^0 \rightarrow \mu^+ \mu^- K^{*0}$ decays we use the world average measured branching ratios [23], while for $B_s^0 \rightarrow \mu^+ \mu^- \phi$ we use the theoretical estimate [15]. The expected number of background events, N_{bkg} , is estimated by extrapolating the candidate yield with an invariant mass $(180 - 300) \text{ MeV}/c^2$ higher than the B mass, to the signal region. Candidates with an invariant mass lower than the B mass are not suitable for background estimates, since they contain partially reconstructed B decays, not expected in the signal region. We find good discriminating power between signal and background from the following three quantities: t/σ_t , α , and I . The significance of the proper decay time, t/σ_t , is defined as the proper decay time of the B candidate, divided by its uncertainty. The angle α is defined as the difference in angle between the B candidate's momentum vector and the vector from the primary vertex to the $\mu\mu h$ vertex. The isolation, I , is defined as the transverse momentum carried by the B meson candidate divided by the transverse momentum of all tracks in a cone of $\Delta R = \sqrt{\Delta\eta^2 + \Delta\phi^2} = 1.0$ around the direction of the B meson candidate, including those of the B candidate itself. Here $\Delta\eta$ is the difference in pseudorapidity of the B candidate and each track, and $\Delta\phi$ is the difference in their azimuthal angles. Scanning different combinations of selection thresholds, we find that the optimal values are very similar for the three rare decay modes: $t/\sigma_t \geq 14$, $\alpha \leq 60 \text{ mrad}$, and $I \geq 0.6$. Applying the optimized selection requirements to the normalization channels yields the distributions shown in Fig. 1. The shape of the combinatoric background is estimated from a sample with poor vertex quality (χ^2 probability $< 10^{-3}$). The invariant mass distribution of this poor vertex quality sample is fitted with a Gaussian distribution for the remaining signal contribution and an exponential plus a constant to model the background. We estimate the background in the signal region of the tight selection using this functional form, normalized to the number of candidates with invariant mass $(60 - 180) \text{ MeV}/c^2$ higher than the B mass. Using this method, we find $6361 \pm 82 B^+ \rightarrow J/\psi K^+$, $2423 \pm 52 B^0 \rightarrow J/\psi K^{*0}$, and $431 \pm 22 B_s^0 \rightarrow J/\psi \phi$ decays. The invariant mass distributions for the rare decay modes are shown in Fig. 2. In the $\pm 40 \text{ MeV}/c^2$ window around the B mass we find 90 $B^+ \rightarrow \mu^+ \mu^- K^+$, 35 $B^0 \rightarrow \mu^+ \mu^- K^{*0}$, and 11 $B_s^0 \rightarrow \mu^+ \mu^- \phi$ candidates. From simulation studies we verified that the present selection accepts decays for every kinematically possible dimuon invariant mass, with an efficiency difference not exceeding a factor two, except for the windows around the $J/\psi^{(\prime)}$ that have been explicitly excluded.

For the signal modes, we evaluate three sources of background: the combinatoric background, hadrons misidentified as muons, and hadrons with misassigned mass. As in the normalization mode, the shape of the combinatoric background is estimated from a sample with poor vertex quality (χ^2 probability $< 10^{-3}$). The

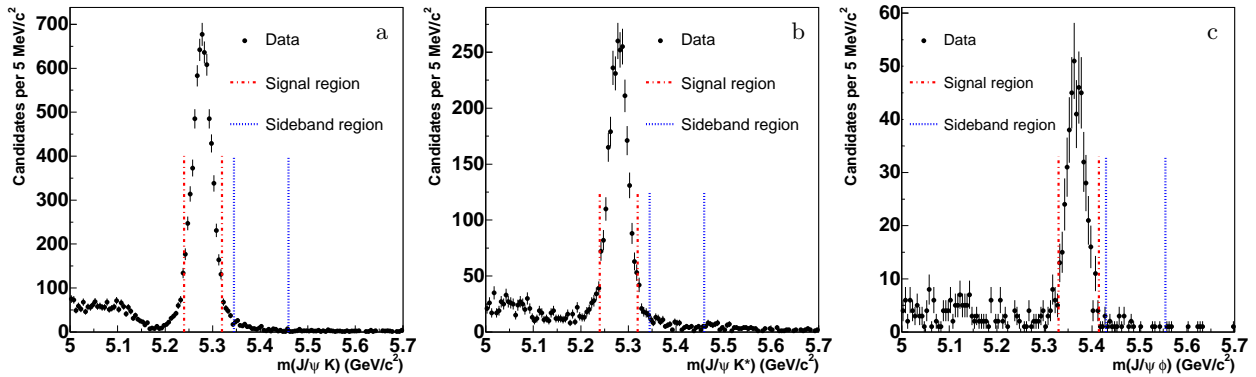


FIG. 1: Invariant mass spectra of (a) $J/\psi K^+$, (b) $J/\psi K^{*0}$ and (c) $J/\psi \phi$ candidates after applying optimized selection requirements.

invariant mass distribution of these candidates is fitted to an exponential plus a constant. This functional form is used to extrapolate the number of candidates with invariant mass ($60 - 180$) MeV/c^2 higher than the B mass to the signal region. The resulting backgrounds, and their statistical uncertainties, consist of 44.3 ± 5.8 , 16.3 ± 3.6 , and 3.1 ± 1.5 candidates for the $B^+ \rightarrow \mu^+ \mu^- K^+$, $B^0 \rightarrow \mu^+ \mu^- K^{*0}$, and $B_s^0 \rightarrow \mu^+ \mu^- \phi$ decay modes, respectively. Backgrounds from hadrons misidentified as muons are estimated from simulation. Final state particles from simulated charmless B decays are weighted with the muon misidentification probabilities. The misidentification probabilities for charged kaons and pions are measured from a sample of $D^{*+} \rightarrow D^0 \pi^+$ followed by $D^0 \rightarrow K^- \pi^+$ decays. We estimate a net background of 1.0 events for the $B^+ \rightarrow \mu^+ \mu^- K^+$ channel, primarily coming from misidentified $B^+ \rightarrow K^+ \pi^- \pi^+$ decays. For the B^0 and B_s^0 modes, this background is negligible. From simulation we determine the background contribution that arises from assigning the wrong masses to the hadrons. We estimate 0.4 $B^0 \rightarrow \mu^+ \mu^- K^{*0}$ decays which are reconstructed as $B_s^0 \rightarrow \mu^+ \mu^- \phi$ and 0.2 $B_s^0 \rightarrow \mu^+ \mu^- \phi$ decays reconstructed as $B^0 \rightarrow \mu^+ \mu^- K^{*0}$.

We calculate the signal yield by subtracting the predicted background from the number of candidates in the signal window. We find an excess in the B signal region in all three channels, and determine the significance by calculating the Poisson probability for the background to fluctuate to the number of observed events or higher, taking into account the uncertainty on the background. We find an equivalent Gaussian significance of 4.5, 2.9, and 2.4 standard deviations, respectively for the B^+ , B^0 , and B_s^0 modes.

Table I lists the systematic uncertainties associated with the relative selection efficiency, discussed in further detail below. To take into account the uncertainty on the relative efficiency due to uncertainties in the dynamics of the rare decays, we apply the weak form factors from Ref. [28, 29] and evaluate the largest difference between the reconstruction efficiency and the cen-

tral value. We find an uncertainty of 3.1% or less. The uncertainty related to the $p_T(B)$ spectrum is evaluated from the change in relative efficiency when the three parameters in the $p_T(B)$ weighting function are varied by one standard deviation of their values determined from fits to data, taking into account correlations. The difference reaches 1.4% in the B_s^0 mode. The muon trigger efficiency close to the 1.5 GeV/c p_T threshold is poorly known. We find a change in the relative efficiency reaching 1.3% if the minimum p_T is varied by $\pm 100 \text{ MeV}/c$, covering the range over which the trigger efficiency rises from zero to one. The final state particles of the rare decay modes have approximately 10% more low momentum tracks than those of the normalization channels. The simulation models the track reconstruction efficiency to an accuracy of 2% in the p_T range of 0.4–1.5 GeV/c . We therefore assign a systematic uncertainty on the relative efficiency of $2\% \times 10\% = 0.2\%$. We find an uncertainty of 8.3% on the relative efficiency of B_s^0 decays due to the unknown fraction of the short-lived CP-even state in the rare decay mode. We assume that the CP-even fraction is 0.5, and assess systematic uncertainties for the extremes of the fraction valued at 1.0 and 0.0. In addition, the uncertainty on $\Delta\Gamma/\Gamma$ contributes another 2.6%, resulting in a total uncertainty of 8.7% associated with the B_s^0 decay width difference. This is the largest systematic uncertainty on the relative efficiency of the B_s^0 mode. We evaluate the effect of the uncertainty on the fraction of J/ψ mesons produced with a longitudinal polarization by varying the fraction measured at CDF [26] by $\pm 1\sigma$. The effect is 0.6% for $B^0 \rightarrow J/\psi K^{*0}$ and 0.1% for $B_s^0 \rightarrow J/\psi \phi$.

The statistical uncertainties of yields in the normalization channels are included as systematic uncertainties, which range from 1.3% for the B^+ channel to 5.1% for the B_s^0 channel. Cabibbo-suppressed $B^+ \rightarrow J/\psi \pi^+$ decays contribute 0.1% to the yield of the normalization channel for the B^+ channel. We introduce the full effect into our estimate of the systematic uncertainty without correcting the result. The relative efficiencies between signal

TABLE I: Systematic uncertainties on the relative efficiency quoted in percent.

Channel	B^+	B^0	B_s
Theory model	1.5	3.1	1.6
$p_T(B)$ spectrum	0.6	1.3	1.4
Trigger turn-on	1.3	1.3	1.2
Low momentum hadrons	0.2	0.2	0.2
B_s^0 decay width difference	–	–	8.7
Polarization	–	0.6	0.1
Norm. channel statistics	1.3	2.1	5.1
$B^+ \rightarrow J/\psi\pi^+$ contribution	0.1	–	–
MC statistics	1.6	2.6	2.2
Total	2.9	5.0	10.6

TABLE II: Summary of systematic uncertainties quoted in percent.

Channel	B^+	B^0	B_s
Total rel. eff. uncertainty	2.9	5.0	10.6
$\mathcal{B}(J/\psi \rightarrow \mu^+\mu^-)$	1.0	1.0	1.0
Background prediction	5.2	3.1	10.2
$\mathcal{B}(B \rightarrow J/\psi h)$	3.5	4.5	35.5

and normalization channels, of 0.71 ± 0.01 , 0.74 ± 0.02 , and 0.84 ± 0.02 for the B^+ , B^0 , and B_s^0 decays, respectively, have uncertainties reaching 2.6%, that arise from the finite size of the MC samples.

The predicted background values depend on the shape of the background function. We evaluate the change in the background yield calculation when using a sample that is similar to the one resulting from the optimal selection, but has less stringent requirements on the three optimization variables instead of the default sample with poor vertex quality. We compare two functional models for the background description, the default exponential plus a constant, and a simpler linear extrapolation function. We find a systematic uncertainty on the background prediction reaching 10% for the B_s^0 channel.

To calculate the systematic uncertainty on the relative branching fraction, the relative efficiency uncertainty is summed in quadrature with the uncertainty of the $J/\psi \rightarrow \mu^+\mu^-$ branching ratio, and with the systematic uncertainty on the number of signal candidates.

To calculate the absolute branching fractions, we use the world average branching fractions of the normalization channels [23]. These branching fractions have uncertainties of 3.5%, 4.5%, and 35.5%, respectively, for B^+ , B^0 , and B_s^0 , which are added in quadrature to the systematic uncertainties on the relative branching ratios. A summary of the systematic uncertainties is given in Table II.

We calculate relative branching ratios using Eq. (1), and find $\mathcal{B}(B^+ \rightarrow \mu^+\mu^-K^+)/\mathcal{B}(B^+ \rightarrow J/\psi K^+) = (0.59 \pm 0.15 \pm 0.03) \times 10^{-3}$, $\mathcal{B}(B^0 \rightarrow \mu^+\mu^-K^{*0})/\mathcal{B}(B^0 \rightarrow$

$J/\psi K^{*0}) = (0.61 \pm 0.23 \pm 0.07) \times 10^{-3}$, and $\mathcal{B}(B_s^0 \rightarrow \mu^+\mu^-\phi)/\mathcal{B}(B_s^0 \rightarrow J/\psi\phi) = (1.23 \pm 0.60 \pm 0.14) \times 10^{-3}$, where the first uncertainty is statistical, and the second is systematic. We use the world-average branching ratios of the B^0 and B^+ normalization channels [23], resulting in the following absolute branching fractions: $\mathcal{B}(B^+ \rightarrow \mu^+\mu^-K^+) = (0.59 \pm 0.15 \pm 0.04) \times 10^{-6}$, and $\mathcal{B}(B^0 \rightarrow \mu^+\mu^-K^{*0}) = (0.81 \pm 0.30 \pm 0.10) \times 10^{-6}$. To obtain an absolute branching ratio for the $B_s^0 \rightarrow \mu^+\mu^-\phi$ decay, we use $\mathcal{B}(B_s^0 \rightarrow J/\psi\phi) = (1.38 \pm 0.49) \times 10^{-3}$, obtained from correcting the CDF measurement [30] for the current value of f_s/f_d [23], the B_s^0 to B^0 production ratio, resulting in $\mathcal{B}(B_s^0 \rightarrow \mu^+\mu^-\phi) = (1.70 \pm 0.82 \pm 0.64) \times 10^{-6}$. We find a significance of only 2.4 standard deviations for the $B_s^0 \rightarrow \mu^+\mu^-\phi$ decay mode. Therefore, we choose to set a limit on this decay. We use a Bayesian integration assuming a flat prior [31], and find $\mathcal{B}(B_s^0 \rightarrow \mu^+\mu^-\phi)/\mathcal{B}(B_s^0 \rightarrow J/\psi\phi) < 2.6(2.3) \times 10^{-3}$ at the 95(90)% confidence level (C.L.). We also set an upper limit on the absolute branching ratio, taking into account the uncertainty of the branching ratio of the normalization channel [32]. We assume that the prior probability density function representing the uncertainty in the normalization channel is a log normal distribution with a mean equal to the central value, and a width parameter equal to the quoted uncertainty of 35.5%. We obtain $\mathcal{B}(B_s^0 \rightarrow \mu^+\mu^-\phi) < 6.0(5.0) \times 10^{-6}$ at 95(90)% C.L. The main ingredients and the results are summarized in Table III.

In conclusion, our measurements of the B^+ and B^0 rare decay modes are consistent with the SM predictions, and with previous measurements [5, 6]. The relative limit on $B_s^0 \rightarrow \mu^+\mu^-\phi$ is consistent with the SM predictions, and is the most stringent to date.

Acknowledgments

We thank the Fermilab staff and the technical staffs of the participating institutions for their vital contributions. This work was supported by the U.S. Department of Energy and National Science Foundation; the Italian Istituto Nazionale di Fisica Nucleare; the Ministry of Education, Culture, Sports, Science and Technology of Japan; the Natural Sciences and Engineering Research Council of Canada; the National Science Council of the Republic of China; the Swiss National Science Foundation; the A.P. Sloan Foundation; the Bundesministerium für Bildung und Forschung, Germany; the Korean Science and Engineering Foundation and the Korean Research Foundation; the Science and Technology Facilities Council and the Royal Society, UK; the Institut National de Physique Nucleaire et Physique des Particules/CNRS; the Russian Foundation for Basic Research; the Comisión Interministerial de Ciencia y Tecnología, Spain; the European Community's Human Potential Programme; the Slovak R&D Agency; and the Academy of Finland.

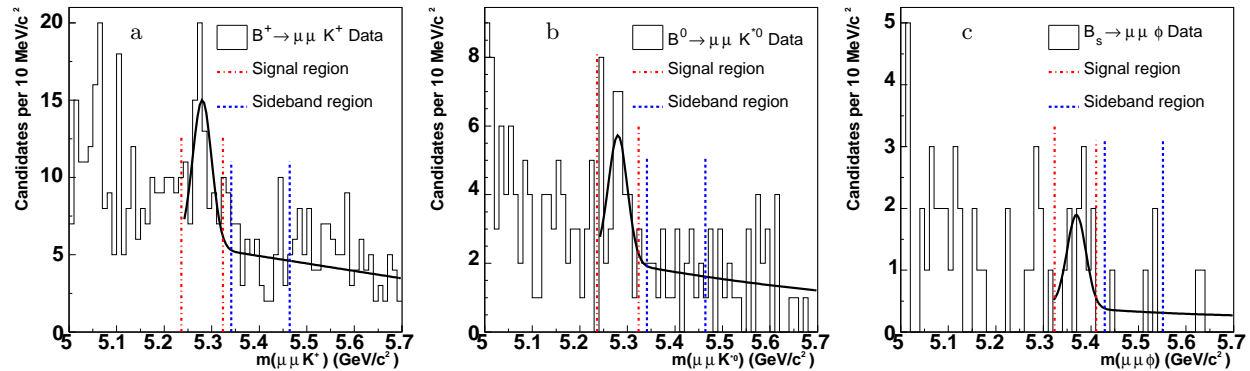


FIG. 2: Invariant mass spectra of (a) $\mu^+\mu^-K^+$, (b) $\mu^+\mu^-K^{*0}$ and (c) $\mu^+\mu^-\phi$ candidates. The superimposed curves are a sum of a single Gaussian with a width of $20 \text{ MeV}/c^2$ representing the signal, and a curve representing the background as determined by the procedure described in the text. The curves are not drawn for masses below the signal window, since they are not expected to predict the background level where partially reconstructed B decays contribute.

TABLE III: Summary of the main ingredients and results of this analysis. Where one uncertainty is quoted, the uncertainty is of statistical nature. Where two uncertainties are quoted, the first is statistical, and the second is systematic.

Decay mode	$B^+ \rightarrow \mu^+\mu^-K^+$	$B^0 \rightarrow \mu^+\mu^-K^{*0}$	$B_s^0 \rightarrow \mu^+\mu^-\phi$
N_{obs}	90	35	11
N_{bkg}	45.3 ± 5.8	16.5 ± 3.6	3.5 ± 1.5
N_{sig}	44.7 ± 5.8	18.5 ± 3.6	7.5 ± 1.5
Gaussian significance	4.5σ	2.9σ	2.4σ
$N_{J/\psi h}$	6361 ± 82	2423 ± 52	431 ± 22
$\epsilon_{\mu^+\mu^-h}/\epsilon_{J/\psi h}$	0.71 ± 0.01	0.74 ± 0.02	0.84 ± 0.02
Rel $\mathcal{B} \times 10^3$	$0.59 \pm 0.15 \pm 0.03$	$0.61 \pm 0.23 \pm 0.07$	$1.23 \pm 0.60 \pm 0.14$
Abs $\mathcal{B} \times 10^6$	$0.59 \pm 0.15 \pm 0.04$	$0.81 \pm 0.30 \pm 0.10$	$1.70 \pm 0.82 \pm 0.64$
Rel \mathcal{B} 95(90)%C.L. limit $\times 10^3$	—	—	2.6(2.3)
Abs \mathcal{B} 95(90)%C.L. limit $\times 10^6$	—	—	6.0(5.0)

- [1] P. Colangelo, F. De Fazio, R. Ferrandes, and T. N. Pham, Phys. Rev. D **73**, 115006 (2006).
- [2] F. Kruger and J. Matias, Phys. Rev. D **71**, 094009 (2005).
- [3] T. M. Aliev, A. Ozpineci, and M. Savci, Eur. Phys. J. C **29**, 265 (2003).
- [4] D. A. Demir, K. A. Olive, and M. B. Voloshin, Phys. Rev. D **66**, 034015 (2002).
- [5] B. Aubert *et al.* (BABAR Collaboration), Phys. Rev. D **73**, 092001 (2006).
- [6] A. Ishikawa *et al.* (Belle Collaboration), Phys. Rev. Lett. **91**, 261601 (2003).
- [7] G. Burdman, Phys. Rev. D **52**, 6400 (1995)
- [8] P. Colangelo, F. De Fazio, P. Santorelli, and E. Scrimieri, Phys. Rev. D **53**, 3672 (1996) [Erratum-ibid. D **57**, 3186 (1998)]
- [9] T. M. Aliev, A. Ozpineci, and M. Savci, Phys. Rev. D **56**, 4260 (1997)
- [10] D. Melikhov, N. Nikitin, and S. Simula, Phys. Rev. D **57**, 6814 (1998)
- [11] A. Ali, P. Ball, L. T. Handoko, and G. Hiller, Phys. Rev. D **61**, 074024 (2000).
- [12] H. M. Choi, C. R. Ji, and L. S. Kisslinger, Phys. Rev. D **65**, 074032 (2002)
- [13] A. Ali, E. Lunghi, C. Greub, and G. Hiller, Phys. Rev. D **66**, 034002 (2002)
- [14] C. H. Chen and C. Q. Geng, Phys. Rev. D **66**, 094018 (2002)
- [15] C. Q. Geng and C. C. Liu, J. Phys. G **29**, 1103 (2003).
- [16] V. M. Abazov *et al.* (D0 Collaboration), Phys. Rev. D **74**, 031107 (2006).
- [17] D. Acosta *et al.* (CDF Collaboration), Phys. Rev. D **65**, 111101 (2002).
- [18] D. Acosta *et al.* (CDF Collaboration), Phys. Rev. D **71**, 032001 (2005).
- [19] A. Sill *et al.*, Nucl. Instrum. Methods A **447**, 1 (2000).
- [20] A. A. Affolder *et al.*, Nucl. Instrum. Methods A **526**, 249 (2004).
- [21] G. Ascoli *et al.*, Nucl. Instrum. Methods A **268**, 33 (1988).
- [22] The CDF reference frame uses cylindrical coordinates, where θ and ϕ are the polar and azimuthal angles with respect to the proton beam. Pseudorapidity η is defined

- as $-\ln(\tan(\theta/2))$.
- [23] W.-M. Yao *et al.*, J. Phys. G **33**, 1 (2006).
 - [24] D. J. Lange, Nucl. Instrum. Methods A **462**, 152 (2001).
 - [25] I. Dunietz, R. Fleischer, and U. Nierste, Phys. Rev. D **63**, 114015 (2001).
 - [26] D. Acosta *et al.* (CDF Collaboration), Phys. Rev. Lett. **94**, 101803 (2005).
 - [27] R. Brun *et al.*, CERN Program Library Long Writeup W5013 (1994).
 - [28] D. Melikhov and B. Stech, Phys. Rev. D **62**, 014006 (2000).
 - [29] P. Colangelo, F. De Fazio, and P. Santorelli, Phys. Rev. D **51**, 2237 (1995).
 - [30] F. Abe *et al.*, (CDF Collaboration), Phys. Rev. D **54**, 6596 (1996).
 - [31] J. Heinrich, C. Blocker, J. Conway, L. Demortier, L. Lyons, G. Punzi, and P. K. Sinervo, arXiv:physics/0409129.
 - [32] Note that the uncertainty in the normalization mode's branching ratio was not taken into account in [16].

Search for the Rare Decays $B^+ \rightarrow \mu^+ \mu^- K^+$, $B^0 \rightarrow \mu^+ \mu^- K^*(892)^0$, and $B_s^0 \rightarrow \mu^+ \mu^- \phi$ at CDF

T. Aaltonen,²⁴ J. Adelman,¹⁴ T. Akimoto,⁵⁶ M.G. Albrow,¹⁸ B. Álvarez González,¹² S. Amerio^u,⁴⁴ D. Amidei,³⁵ A. Anastassov,³⁹ A. Annovi,²⁰ J. Antos,¹⁵ G. Apollinari,¹⁸ A. Apresyan,⁴⁹ T. Arisawa,⁵⁸ A. Artikov,¹⁶ W. Ashmanskas,¹⁸ A. Attal,⁴ A. Aurisano,⁵⁴ F. Azfar,⁴³ P. Azzurri^s,⁴⁷ W. Badgett,¹⁸ A. Barbaro-Galtieri,²⁹ V.E. Barnes,⁴⁹ B.A. Barnett,²⁶ V. Bartsch,³¹ G. Bauer,³³ P.-H. Beauchemin,³⁴ F. Bedeschi,⁴⁷ P. Bednar,¹⁵ D. Beecher,³¹ S. Behari,²⁶ G. Bellettini^q,⁴⁷ J. Bellinger,⁶⁰ D. Benjamin,¹⁷ A. Beretvas,¹⁸ J. Beringer,²⁹ A. Bhatti,⁵¹ M. Binkley,¹⁸ D. Bisello^u,⁴⁴ I. Bizjak,³¹ R.E. Blair,² C. Blocker,⁷ B. Blumenfeld,²⁶ A. Bocci,¹⁷ A. Bodek,⁵⁰ V. Boisvert,⁵⁰ G. Bolla,⁴⁹ D. Bortoletto,⁴⁹ J. Boudreau,⁴⁸ A. Boveia,¹¹ B. Brau,¹¹ A. Bridgeman,²⁵ L. Brigliadori,⁴⁴ C. Bromberg,³⁶ E. Brubaker,¹⁴ J. Budagov,¹⁶ H.S. Budd,⁵⁰ S. Budd,²⁵ K. Burkett,¹⁸ G. Busetto^u,⁴⁴ P. Bussey^x,²² A. Buzatu,³⁴ K. L. Byrum,² S. Cabrera^p,¹⁷ C. Calancha,³² M. Campanelli,³⁶ M. Campbell,³⁵ F. Canelli,¹⁸ A. Canepa,⁴⁶ D. Carlsmith,⁶⁰ R. Carosi,⁴⁷ S. Carrillo^j,¹⁹ S. Carron,³⁴ B. Casal,¹² M. Casarsa,¹⁸ A. Castro^t,⁶ P. Catastini^r,⁴⁷ D. Cauz^w,⁵⁵ V. Cavaliere^r,⁴⁷ M. Cavalli-Sforza,⁴ A. Cerri,²⁹ L. Cerritoⁿ,³¹ S.H. Chang,²⁸ Y.C. Chen,¹ M. Chertok,⁸ G. Chiarelli,⁴⁷ G. Chlachidze,¹⁸ F. Chlebana,¹⁸ K. Cho,²⁸ D. Chokheli,¹⁶ J.P. Chou,²³ G. Choudalakis,³³ S.H. Chuang,⁵³ K. Chung,¹³ W.H. Chung,⁶⁰ Y.S. Chung,⁵⁰ C.I. Ciobanu,⁴⁵ M.A. Ciocci^r,⁴⁷ A. Clark,²¹ D. Clark,⁷ G. Compostella,⁴⁴ M.E. Convery,¹⁸ J. Conway,⁸ K. Copic,³⁵ M. Cordelli,²⁰ G. Cortiana^u,⁴⁴ D.J. Cox,⁸ F. Crescioli^q,⁴⁷ C. Cuenca Almenar^p,⁸ J. Cuevas^m,¹² R. Culbertson,¹⁸ J.C. Cully,³⁵ D. Dagenhart,¹⁸ M. Datta,¹⁸ T. Davies,²² P. de Barbaro,⁵⁰ S. De Cecco,⁵² A. Deisher,²⁹ G. De Lorenzo,⁴ M. Dell'Orso^q,⁴⁷ C. Deluca,⁴ L. Demortier,⁵¹ J. Deng,¹⁷ M. Deninno,⁶ P.F. Derwent,¹⁸ G.P. di Giovanni,⁴⁵ C. Dionisi^v,⁵² B. Di Ruzza^w,⁵⁵ J.R. Dittmann,⁵ M. D'Onofrio,⁴ S. Donati^q,⁴⁷ P. Dong,⁹ J. Donini,⁴⁴ T. Dorigo,⁴⁴ S. Dube,⁵³ J. Efron,⁴⁰ A. Elagin,⁵⁴ R. Erbacher,⁸ D. Errede,²⁵ S. Errede,²⁵ R. Eusebi,¹⁸ H.C. Fang,²⁹ S. Farrington,⁴³ W.T. Fedorko,¹⁴ R.G. Feild,⁶¹ M. Feindt,²⁷ J.P. Fernandez,³² C. Ferrazza^s,⁴⁷ R. Field,¹⁹ G. Flanagan,⁴⁹ R. Forrest,⁸ M. Franklin,²³ J.C. Freeman,¹⁸ I. Furic,¹⁹ M. Gallinaro,⁵² J. Galyardt,¹³ F. Garbersen,¹¹ J.E. Garcia,⁴⁷ A.F. Garfinkel,⁴⁹ K. Genser,¹⁸ H. Gerberich,²⁵ D. Gerdes,³⁵ A. Gessler,²⁷ S. Giagu^v,⁵² V. Giakoumopoulou,³ P. Giannetti,⁴⁷ K. Gibson,⁴⁸ J.L. Gimmell,⁵⁰ C.M. Ginsburg,¹⁸ N. Giokaris,³ M. Giordani^w,⁵⁵ P. Giromini,²⁰ M. Giunta^q,⁴⁷ G. Giurgiu,²⁶ V. Glagolev,¹⁶ D. Glenzinski,¹⁸ M. Gold,³⁸ N. Goldschmidt,¹⁹ A. Golossanov,¹⁸ G. Gomez,¹² G. Gomez-Ceballos,³³ M. Goncharov,⁵⁴ O. González,³² I. Gorelov,³⁸ A.T. Goshaw,¹⁷ K. Goulianos,⁵¹ A. Gresele^u,⁴⁴ S. Grinstein,²³ C. Grosso-Pilcher,¹⁴ R.C. Group,¹⁸ U. Grundler,²⁵ J. Guimaraes da Costa,²³ Z. Gunay-Unalan,³⁶ C. Haber,²⁹ K. Hahn,³³ S.R. Hahn,¹⁸ E. Halkiadakis,⁵³ B.-Y. Han,⁵⁰ J.Y. Han,⁵⁰ R. Handler,⁶⁰ F. Happacher,²⁰ K. Hara,⁵⁶ D. Hare,⁵³ M. Hare,⁵⁷ S. Harper,⁴³ R.F. Harr,⁵⁹ R.M. Harris,¹⁸ M. Hartz,⁴⁸ K. Hatakeyama,⁵¹ J. Hauser,⁹ C. Hays,⁴³ M. Heck,²⁷ A. Heijboer,⁴⁶ B. Heinemann,²⁹ J. Heinrich,⁴⁶ C. Henderson,³³ M. Herndon,⁶⁰ J. Heuser,²⁷ S. Hewamanage,⁵ D. Hidas,¹⁷ C.S. Hill^c,¹¹ D. Hirschbuehl,²⁷ A. Hocker,¹⁸ S. Hou,¹ M. Houlden,³⁰ S.-C. Hsu,¹⁰ B.T. Huffman,⁴³ R.E. Hughes,⁴⁰ U. Husemann,⁶¹ J. Huston,³⁶ J. Incandela,¹¹ G. Introzzi,⁴⁷ M. Iori^v,⁵² A. Ivanov,⁸ E. James,¹⁸ B. Jayatilaka,¹⁷ E.J. Jeon,²⁸ M.K. Jha,⁶ S. Jindariani,¹⁸ W. Johnson,⁸ M. Jones,⁴⁹ K.K. Joo,²⁸ S.Y. Jun,¹³ J.E. Jung,²⁸ T.R. Junk,¹⁸ T. Kamon,⁵⁴ D. Kar,¹⁹ P.E. Karchin,⁵⁹ Y. Kato,⁴² R. Kephart,¹⁸ J. Keung,⁴⁶ V. Khotilovich,⁵⁴ B. Kilminster,⁴⁰ D.H. Kim,²⁸ H.S. Kim,²⁸ J.E. Kim,²⁸ M.J. Kim,²⁰ S.B. Kim,²⁸ S.H. Kim,⁵⁶ Y.K. Kim,¹⁴ N. Kimura,⁵⁶ L. Kirsch,⁷ S. Klimentenko,¹⁹ B. Knuteson,³³ B.R. Ko,¹⁷ S.A. Koay,¹¹ K. Kondo,⁵⁸ D.J. Kong,²⁸ J. Konigsberg,¹⁹ A. Korytov,¹⁹ A.V. Kotwal,¹⁷ M. Kreps,²⁷ J. Kroll,⁴⁶ N. Krumnack,⁵ M. Kruse,¹⁷ V. Krutelyov,¹¹ T. Kubo,⁵⁶ T. Kuhr,²⁷ N.P. Kulkarni,⁵⁹ M. Kurata,⁵⁶ Y. Kusakabe,⁵⁸ S. Kwang,¹⁴ A.T. Laasanen,⁴⁹ S. Lami,⁴⁷ S. Lammel,¹⁸ M. Lancaster,³¹ R.L. Lander,⁸ K. Lannon,⁴⁰ A. Lath,⁵³ G. Latino^r,⁴⁷ I. Lazzizzera^u,⁴⁴ T. LeCompte,² E. Lee,⁵⁴ S.W. Lee^o,⁵⁴ S. Leone,⁴⁷ S. Levy,¹⁴ J.D. Lewis,¹⁸ C.S. Lin,²⁹ J. Linacre,⁴³ M. Lindgren,¹⁸ E. Lipeles,¹⁰ A. Lister,⁸ D.O. Litvintsev,¹⁸ C. Liu,⁴⁸ T. Liu,¹⁸ N.S. Lockyer,⁴⁶ A. Loginov,⁶¹ M. Loretini^u,⁴⁴ L. Lovas,¹⁵ R.-S. Lu,¹ D. Lucchesi^u,⁴⁴ J. Lueck,²⁷ C. Luci^v,⁵² P. Lujan,²⁹ P. Lukens,¹⁸ G. Lungu,⁵¹ L. Lyons,⁴³ J. Lys,²⁹ R. Lysak,¹⁵ E. Lytken,⁴⁹ P. Mack,²⁷ D. MacQueen,³⁴ R. Madrak,¹⁸ K. Maeshima,¹⁸ K. Makhoul,³³ T. Maki,²⁴ P. Maksimovic,²⁶ S. Malde,⁴³ S. Malik,³¹ G. Manca,³⁰ A. Manousakis-Katsikakis,³ F. Margaroli,⁴⁹ C. Marino,²⁷ C.P. Marino,²⁵ A. Martin,⁶¹ V. Martinⁱ,²² M. Martínez,⁴ R. Martínez-Ballarín,³² T. Maruyama,⁵⁶ P. Mastrandrea,⁵² T. Masubuchi,⁵⁶ M.E. Mattson,⁵⁹ P. Mazzanti,⁶ K.S. McFarland,⁵⁰ P. McIntyre,⁵⁴ R. McNulty,^h,³⁰ A. Mehta,³⁰ P. Mehtala,²⁴ A. Menzione,⁴⁷ P. Merkel,⁴⁹ C. Mesropian,⁵¹ T. Miao,¹⁸ N. Miladinovic,⁷ R. Miller,³⁶ C. Mills,²³ M. Milnik,²⁷ A. Mitra,¹ G. Mitselmakher,¹⁹ H. Miyake,⁵⁶ N. Moggi,⁶ C.S. Moon,²⁸ R. Moore,¹⁸ M.J. Morello^q,⁴⁷ J. Morlok,²⁷ P. Movilla Fernandez,¹⁸ J. Mülmenstädt,²⁹ A. Mukherjee,¹⁸ Th. Muller,²⁷ R. Mumford,²⁶ P. Murat,¹⁸ M. Mussini^t,⁶ J. Nachtman,¹⁸ Y. Nagai,⁵⁶ A. Nagano,⁵⁶ J. Naganoma,⁵⁸ K. Nakamura,⁵⁶ I. Nakano,⁴¹ A. Napier,⁵⁷ V. Necula,¹⁷ C. Neu,⁴⁶

M.S. Neubauer,²⁵ J. Nielsen^e,²⁹ L. Nodulman,² M. Norman,¹⁰ O. Norriella,²⁵ E. Nurse,³¹ L. Oakes,⁴³ S.H. Oh,¹⁷ Y.D. Oh,²⁸ I. Oksuzian,¹⁹ T. Okusawa,⁴² R. Oldeman,³⁰ R. Orava,²⁴ K. Osterberg,²⁴ S. Pagan Griso^u,⁴⁴ C. Pagliarone,⁴⁷ E. Palencia,¹⁸ V. Papadimitriou,¹⁸ A. Papaikononou,²⁷ A.A. Paramonov,¹⁴ B. Parks,⁴⁰ S. Pashapour,³⁴ J. Patrick,¹⁸ G. Pauletta^w,⁵⁵ M. Paulini,¹³ C. Paus,³³ D.E. Pellett,⁸ A. Penzo,⁵⁵ T.J. Phillips,¹⁷ G. Piacentino,⁴⁷ E. Pianori,⁴⁶ L. Pinera,¹⁹ K. Pitts,²⁵ C. Plager,⁹ L. Pondrom,⁶⁰ O. Poukhov,¹⁶ N. Pounder,⁴³ F. Prakhoshyn,¹⁶ A. Pronko,¹⁸ J. Proudfoot,² F. Ptohos^g,¹⁸ E. Pueschel,¹³ G. Punzi^q,⁴⁷ J. Pursley,⁶⁰ J. Rademacker^c,⁴³ A. Rahaman,⁴⁸ V. Ramakrishnan,⁶⁰ N. Ranjan,⁴⁹ I. Redondo,³² B. Reisert,¹⁸ V. Rekovic,³⁸ P. Renton,⁴³ M. Rescigno,⁵² S. Richter,²⁷ F. Rimondi^t,⁶ L. Ristori,⁴⁷ A. Robson,²² T. Rodrigo,¹² T. Rodriguez,⁴⁶ E. Rogers,²⁵ S. Rolli,⁵⁷ R. Roser,¹⁸ M. Rossi,⁵⁵ R. Rossin,¹¹ P. Roy,³⁴ A. Ruiz,¹² J. Russ,¹³ V. Rusu,¹⁸ H. Saarikko,²⁴ A. Safonov,⁵⁴ W.K. Sakumoto,⁵⁰ O. Saltó,⁴ L. Santi^w,⁵⁵ S. Sarkar^v,⁵² L. Sartori,⁴⁷ K. Sato,¹⁸ A. Savoy-Navarro,⁴⁵ T. Scheidle,²⁷ P. Schlabach,¹⁸ A. Schmidt,²⁷ E.E. Schmidt,¹⁸ M.A. Schmidt,¹⁴ M.P. Schmidt^{*},⁶¹ M. Schmitt,³⁹ T. Schwarz,⁸ L. Scodellaro,¹² A.L. Scott,¹¹ A. Scribano^r,⁴⁷ F. Scuri,⁴⁷ A. Sedov,⁴⁹ S. Seidel,³⁸ Y. Seiya,⁴² A. Semenov,¹⁶ L. Sexton-Kennedy,¹⁸ A. Sfyra,²¹ S.Z. Shalhout,⁵⁹ T. Shears,³⁰ P.F. Shepard,⁴⁸ D. Sherman,²³ M. Shimojima^l,⁵⁶ S. Shiraiishi,¹⁴ M. Shochet,¹⁴ Y. Shon,⁶⁰ I. Shreyber,³⁷ A. Sidoti,⁴⁷ P. Sinervo,³⁴ A. Sisakyan,¹⁶ A.J. Slaughter,¹⁸ J. Slaunwhite,⁴⁰ K. Sliwa,⁵⁷ J.R. Smith,⁸ F.D. Snider,¹⁸ R. Snihur,³⁴ A. Soha,⁸ S. Somalwar,⁵³ V. Sorin,³⁶ J. Spalding,¹⁸ T. Spreitzer,³⁴ P. Squillacioti^r,⁴⁷ M. Stanitzki,⁶¹ R. St. Denis,²² B. Stelzer,⁹ O. Stelzer-Chilton,⁴³ D. Stentz,³⁹ J. Strologas,³⁸ D. Stuart,¹¹ J.S. Suh,²⁸ A. Sukhanov,¹⁹ I. Suslov,¹⁶ T. Suzuki,⁵⁶ A. Taffard^d,²⁵ R. Takashima,⁴¹ Y. Takeuchi,⁵⁶ R. Tanaka,⁴¹ M. Tecchio,³⁵ P.K. Teng,¹ K. Terashi,⁵¹ R.J. Tesarek,¹⁸ J. Thom^f,¹⁸ A.S. Thompson,²² G.A. Thompson,²⁵ E. Thomson,⁴⁶ P. Tipton,⁶¹ V. Tiwari,¹³ S. Tkaczyk,¹⁸ D. Toback,⁵⁴ S. Tokar,¹⁵ K. Tollefson,³⁶ T. Tomura,⁵⁶ D. Tonelli,¹⁸ S. Torre,²⁰ D. Torretta,¹⁸ P. Totaro^w,⁵⁵ S. Tourneur,⁴⁵ Y. Tu,⁴⁶ N. Turini^r,⁴⁷ F. Ukegawa,⁵⁶ S. Vallecorsa,²¹ N. van Remortel^a,²⁴ A. Varganov,³⁵ E. Vataga^s,⁴⁷ F. Vázquez^j,¹⁹ G. Velev,¹⁸ C. Vellidis,³ V. Veszpremi,⁴⁹ M. Vidal,³² R. Vidal,¹⁸ I. Vila,¹² R. Vilar,¹² T. Vine,³¹ M. Vogel,³⁸ I. Volobouev^o,²⁹ G. Volpi^q,⁴⁷ F. Würthwein,¹⁰ P. Wagner,² R.G. Wagner,² R.L. Wagner,¹⁸ J. Wagner-Kuhr,²⁷ W. Wagner,²⁷ T. Wakisaka,⁴² R. Wallny,⁹ S.M. Wang,¹ A. Warburton,³⁴ D. Waters,³¹ M. Weinberger,⁵⁴ W.C. Wester III,¹⁸ B. Whitehouse,⁵⁷ D. Whiteson^d,⁴⁶ A.B. Wicklund,² E. Wicklund,¹⁸ G. Williams,³⁴ H.H. Williams,⁴⁶ P. Wilson,¹⁸ B.L. Winer,⁴⁰ P. Wittich^f,¹⁸ S. Wolbers,¹⁸ C. Wolfe,¹⁴ T. Wright,³⁵ X. Wu,²¹ S.M. Wynne,³⁰ A. Yagil,¹⁰ K. Yamamoto,⁴² J. Yamaoka,⁵³ U.K. Yang^k,¹⁴ Y.C. Yang,²⁸ W.M. Yao,²⁹ G.P. Yeh,¹⁸ J. Yoh,¹⁸ K. Yorita,¹⁴ T. Yoshida,⁴² G.B. Yu,⁵⁰ I. Yu,²⁸ S.S. Yu,¹⁸ J.C. Yun,¹⁸ L. Zanello^v,⁵² A. Zanetti,⁵⁵ I. Zaw,²³ X. Zhang,²⁵ Y. Zheng^b,⁹ and S. Zucchelli^{t6}

(CDF Collaboration[†])

¹*Institute of Physics, Academia Sinica, Taipei, Taiwan 11529, Republic of China*

²*Argonne National Laboratory, Argonne, Illinois 60439*

³*University of Athens, 157 71 Athens, Greece*

⁴*Institut de Fisica d'Altes Energies, Universitat Autònoma de Barcelona, E-08193, Bellaterra (Barcelona), Spain*

⁵*Baylor University, Waco, Texas 76798*

⁶*Istituto Nazionale di Fisica Nucleare Bologna, ^tUniversity of Bologna, I-40127 Bologna, Italy*

⁷*Brandeis University, Waltham, Massachusetts 02254*

⁸*University of California, Davis, Davis, California 95616*

⁹*University of California, Los Angeles, Los Angeles, California 90024*

¹⁰*University of California, San Diego, La Jolla, California 92093*

¹¹*University of California, Santa Barbara, Santa Barbara, California 93106*

¹²*Instituto de Fisica de Cantabria, CSIC-University of Cantabria, 39005 Santander, Spain*

¹³*Carnegie Mellon University, Pittsburgh, PA 15213*

¹⁴*Enrico Fermi Institute, University of Chicago, Chicago, Illinois 60637*

¹⁵*Comenius University, 842 48 Bratislava, Slovakia; Institute of Experimental Physics, 040 01 Kosice, Slovakia*

¹⁶*Joint Institute for Nuclear Research, RU-141980 Dubna, Russia*

¹⁷*Duke University, Durham, North Carolina 27708*

¹⁸*Fermi National Accelerator Laboratory, Batavia, Illinois 60510*

¹⁹*University of Florida, Gainesville, Florida 32611*

²⁰*Laboratori Nazionali di Frascati, Istituto Nazionale di Fisica Nucleare, I-00044 Frascati, Italy*

²¹*University of Geneva, CH-1211 Geneva 4, Switzerland*

²²*Glasgow University, Glasgow G12 8QQ, United Kingdom*

²³*Harvard University, Cambridge, Massachusetts 02138*

²⁴*Division of High Energy Physics, Department of Physics,*

University of Helsinki and Helsinki Institute of Physics, FIN-00014, Helsinki, Finland

²⁵*University of Illinois, Urbana, Illinois 61801*

²⁶*The Johns Hopkins University, Baltimore, Maryland 21218*

²⁷*Institut für Experimentelle Kernphysik, Universität Karlsruhe, 76128 Karlsruhe, Germany*

- ²⁸Center for High Energy Physics: Kyungpook National University, Daegu 702-701, Korea; Seoul National University, Seoul 151-742, Korea; Sungkyunkwan University, Suwon 440-746, Korea; Korea Institute of Science and Technology Information, Daejeon, 305-806, Korea; Chonnam National University, Gwangju, 500-757, Korea
- ²⁹Ernest Orlando Lawrence Berkeley National Laboratory, Berkeley, California 94720
- ³⁰University of Liverpool, Liverpool L69 7ZE, United Kingdom
- ³¹University College London, London WC1E 6BT, United Kingdom
- ³²Centro de Investigaciones Energeticas Medioambientales y Tecnologicas, E-28040 Madrid, Spain
- ³³Massachusetts Institute of Technology, Cambridge, Massachusetts 02139
- ³⁴Institute of Particle Physics: McGill University, Montréal, Canada H3A 2T8; and University of Toronto, Toronto, Canada M5S 1A7
- ³⁵University of Michigan, Ann Arbor, Michigan 48109
- ³⁶Michigan State University, East Lansing, Michigan 48824
- ³⁷Institution for Theoretical and Experimental Physics, ITEP, Moscow 117259, Russia
- ³⁸University of New Mexico, Albuquerque, New Mexico 87131
- ³⁹Northwestern University, Evanston, Illinois 60208
- ⁴⁰The Ohio State University, Columbus, Ohio 43210
- ⁴¹Okayama University, Okayama 700-8530, Japan
- ⁴²Osaka City University, Osaka 588, Japan
- ⁴³University of Oxford, Oxford OX1 3RH, United Kingdom
- ⁴⁴Istituto Nazionale di Fisica Nucleare, Sezione di Padova-Trento, ^uUniversity of Padova, I-35131 Padova, Italy
- ⁴⁵LPNHE, Université Pierre et Marie Curie/IN2P3-CNRS, UMR7585, Paris, F-75252 France
- ⁴⁶University of Pennsylvania, Philadelphia, Pennsylvania 19104
- ⁴⁷Istituto Nazionale di Fisica Nucleare Pisa, ^qUniversity of Pisa, ^rUniversity of Siena and ^sScuola Normale Superiore, I-56127 Pisa, Italy
- ⁴⁸University of Pittsburgh, Pittsburgh, Pennsylvania 15260
- ⁴⁹Purdue University, West Lafayette, Indiana 47907
- ⁵⁰University of Rochester, Rochester, New York 14627
- ⁵¹The Rockefeller University, New York, New York 10021
- ⁵²Istituto Nazionale di Fisica Nucleare, Sezione di Roma 1, ^vSapienza Università di Roma, I-00185 Roma, Italy
- ⁵³Rutgers University, Piscataway, New Jersey 08855
- ⁵⁴Texas A&M University, College Station, Texas 77843
- ⁵⁵Istituto Nazionale di Fisica Nucleare Trieste/ Udine, ^wUniversity of Trieste/ Udine, Italy
- ⁵⁶University of Tsukuba, Tsukuba, Ibaraki 305, Japan
- ⁵⁷Tufts University, Medford, Massachusetts 02155
- ⁵⁸Waseda University, Tokyo 169, Japan
- ⁵⁹Wayne State University, Detroit, Michigan 48201
- ⁶⁰University of Wisconsin, Madison, Wisconsin 53706
- ⁶¹Yale University, New Haven, Connecticut 06520

We search for $b \rightarrow s\mu^+\mu^-$ transitions in B meson (B^+ , B^0 , or B_s^0) decays with 924pb^{-1} of $p\bar{p}$ collisions at $\sqrt{s} = 1.96\text{TeV}$ collected with the CDF II detector at the Fermilab Tevatron. We find excesses with significances of 4.5, 2.9, and 2.4 standard deviations in the $B^+ \rightarrow \mu^+\mu^-K^+$, $B^0 \rightarrow \mu^+\mu^-K^*(892)^0$, and $B_s^0 \rightarrow \mu^+\mu^-\phi$ decay modes, respectively. Using $B \rightarrow J/\psi h$ ($h = K^+$, $K^*(892)^0$, ϕ) decays as normalization channels, we report branching fractions for the previously observed B^+ and B^0 decays, $\mathcal{B}(B^+ \rightarrow \mu^+\mu^-K^+) = (0.59 \pm 0.15 \pm 0.04) \times 10^{-6}$, and $\mathcal{B}(B^0 \rightarrow \mu^+\mu^-K^*(892)^0) = (0.81 \pm 0.30 \pm 0.10) \times 10^{-6}$, where the first uncertainty is statistical, and the second is systematic. These measurements are consistent with the world average results, and are competitive with the best available measurements. We set an upper limit on the relative branching fraction $\frac{\mathcal{B}(B_s^0 \rightarrow \mu^+\mu^-\phi)}{\mathcal{B}(B_s^0 \rightarrow J/\psi\phi)} < 2.6(2.3) \times 10^{-3}$ at the 95(90)% confidence level, which is the most stringent to date.

PACS numbers: Valid PACS appear here

*Deceased

†With visitors from ^aUniversiteit Antwerpen, B-2610 Antwerp, Belgium, ^bChinese Academy of Sciences, Beijing 100864, China, ^cUniversity of Bristol, Bristol BS8 1TL, United Kingdom,

^dUniversity of California Irvine, Irvine, CA 92697, ^eUniversity of California Santa Cruz, Santa Cruz, CA 95064, ^fCornell University, Ithaca, NY 14853, ^gUniversity of Cyprus, Nicosia CY-1678,

The decay of a b quark into an s quark and two muons ($b \rightarrow s\mu^+\mu^-$) is a flavor-changing neutral current process, forbidden at tree level in the standard model (SM) but allowed through highly suppressed internal loops. New physics could manifest itself in a larger branching fraction, a modified dimuon mass distribution, or angular distributions of the decay products different from that predicted by the SM [1–4]. In this paper, we report branching ratio measurements of exclusive decays, where the s quark hadronizes into a single meson. Reconstructing a final state with only three or four charged final state particles results in smaller backgrounds than those expected in a search for inclusive $B \rightarrow X_s\mu^+\mu^-$ decays. The rare decays, $B^+ \rightarrow \mu^+\mu^-K^+$ and $B^0 \rightarrow \mu^+\mu^-K^*(892)^0$ have been observed at the B factories [5, 6], with branching fractions of $O(10^{-6})$, consistent with SM predictions [7–14]. The analogous decay in the B_s^0 system, $B_s^0 \rightarrow \mu^+\mu^-\phi$, has a predicted branching ratio of 1.6×10^{-6} [15], but has not yet been observed [16, 17]. We report branching ratio measurements from 924 pb $^{-1}$ of Collider Detector at Fermilab (CDF) Run II data that pave the way for future studies of larger datasets from which kinematic distributions may be measured. We search for $B \rightarrow \mu^+\mu^-h$ decays, where B stands for B^+ , B^0 , or B_s^0 , and h stands for K^+ , $K^*(892)^0$, or ϕ , respectively. The $K^*(892)^0$, referred to as K^{*0} throughout this paper, is reconstructed in the $K^{*0} \rightarrow K^+\pi^-$, decay mode, and the ϕ meson is reconstructed as $\phi \rightarrow K^+K^-$. We measure branching ratios relative to $B \rightarrow J/\psi h$ decays, followed by $J/\psi \rightarrow \mu^+\mu^-$ decays, resulting in the same final state particles as the rare decay modes. Many systematic uncertainties cancel in the relative branching ratios:

$$\frac{\mathcal{B}(B \rightarrow \mu^+\mu^-h)}{\mathcal{B}(B \rightarrow J/\psi h)} = \frac{N_{\mu^+\mu^-h}}{N_{J/\psi h}} \frac{\epsilon_{J/\psi h}}{\epsilon_{\mu^+\mu^-h}} \times \mathcal{B}(J/\psi \rightarrow \mu^+\mu^-), \quad (1)$$

where $N_{\mu^+\mu^-h}$ is the observed number of $B \rightarrow \mu^+\mu^-h$ decays, $N_{J/\psi h}$ is the observed number of $B \rightarrow J/\psi h$ decays, while $\epsilon_{J/\psi h}$ and $\epsilon_{\mu^+\mu^-h}$ are the combined selection efficiency and acceptance of the experiment for $B \rightarrow J/\psi h$ and $B \rightarrow \mu^+\mu^-h$ respectively. Throughout this report, charge conjugate modes are implicitly included.

CDF II is a general purpose detector, located at the Tevatron $p\bar{p}$ collider [18]. Charged particle trajectories (tracks) are detected by the tracking system comprised of a seven-layer double-sided silicon microstrip detector and

a drift chamber, both in a 1.4 T axial magnetic field. The silicon detector [19] ranges in radius from 1.3 to 28 cm, and has a single-hit resolution of approximately 15 μm . The drift chamber [20] provides up to 96 measurements from radii of 40 to 137 cm with a single-hit resolution of approximately 180 μm . A muon chamber identification system of plastic scintillators and drift chambers [21] is located on the exterior of the detector with a central part covering $|\eta| < 0.6$, and an extended region covering $0.6 < |\eta| < 1.0$, where η is the pseudorapidity [22]. In the central(extended) region, muons are detected if their transverse momentum component, p_T , is greater than 1.5(2.0) GeV/ c . Events are selected with a three-level trigger system. The first trigger level requires the presence of two charged particles with $p_T \geq 1.5$ GeV/ c ($|\eta| \leq 0.6$) or $p_T \geq 2.0$ GeV/ c ($0.6 \leq |\eta| \leq 1.0$), matched to track segments in the muon chambers to form muon candidates. At the second level, a more restrictive selection is made by requiring that the muon candidates have opposite charge, and that their opening angle in the plane transverse to the beamline is less than 120°. At the third trigger level, the event is fully reconstructed. The trajectories of the muon candidates in the silicon detector are required to intersect at a point which is displaced transversely from the beamline by at least 100 μm .

The offline selection begins with a suppression of random combinations of tracks satisfying the selection requirements (combinatoric background), by requiring that all tracks have $p_T > 0.4$ GeV/ c and match hits from at least three layers of the silicon detector. The trajectories of a pair of muon candidates that satisfy the trigger requirements, and the tracks that form the hadron candidate, are fitted with the constraint that they originate from a single vertex in 3-dimensional space to form a B candidate. The χ^2 probability of the fit is required to be greater than 10^{-3} . A K^+ candidate is a track assigned the charged kaon mass, and the K^{*0} (ϕ) candidates are formed from oppositely charged pairs of tracks whose invariant mass must lie within 50 (10) MeV/ c^2 of the K^{*0} (ϕ) mass. For all particles, we use the world average values tabulated in Ref. [23]. The ambiguity of the mass assignment in $B^0 \rightarrow \mu^+\mu^-K^{*0}$ decays is handled by choosing the combination whose $K^+\pi^-$ mass is closer to the K^{*0} mass. In reconstructing the B candidates, the meson containing a strange quark, h , is required to have $p_T(h) \geq 1.0$ GeV/ c , and the B candidate is required to have $p_T(B) \geq 4.0$ GeV/ c . We require that the distance of closest approach between the flight path of the B candidate and the beamline, $|d_0(B)|$, is less than 120 μm , to reduce the combinatoric background with no loss of signal.

Normalization mode candidates are identified by having a dimuon invariant mass within 50 MeV/ c^2 of the J/ψ mass, yielding approximately 12 000 $B^+ \rightarrow J/\psi K^+$, 4400 $B^0 \rightarrow J/\psi K^{*0}$, and 800 $B_s^0 \rightarrow J/\psi \phi$ decays. The B candidate mass distributions of all modes are compatible with a Gaussian of width $\sigma = 20$ MeV/ c^2 . To reduce backgrounds from B decays to mesons contain-

Cyprus, ^hUniversity College Dublin, Dublin 4, Ireland, ⁱUniversity of Edinburgh, Edinburgh EH9 3JZ, United Kingdom, ^jUniversidad Iberoamericana, Mexico D.F., Mexico, ^kUniversity of Manchester, Manchester M13 9PL, England, ^lNagasaki Institute of Applied Science, Nagasaki, Japan, ^mUniversity de Oviedo, E-33007 Oviedo, Spain, ⁿQueen Mary, University of London, London, E1 4NS, England, ^oTexas Tech University, Lubbock, TX 79409, ^pIFIC(CSIC-Universitat de Valencia), 46071 Valencia, Spain, ^xRoyal Society of Edinburgh/Scottish Executive Support Research Fellow,

ing c quarks, several vetoes are applied to $B \rightarrow \mu^+\mu^-h$ candidates, listed below. We eliminate candidates with a dimuon mass near the $J/\psi^{(\prime)}$: $2.9 \leq m_{\mu\mu} \leq 3.2 \text{ GeV}/c^2$ or $3.6 \leq m_{\mu\mu} \leq 3.75 \text{ GeV}/c^2$ respectively. $B \rightarrow J/\psi^{(\prime)}h$ decays followed by the radiative decay of the $J/\psi^{(\prime)}$ into two muons and a photon that is not reconstructed, may have a dimuon mass that passes the $J/\psi^{(\prime)}$ veto. We reject these events making use of the correlation between the candidate's invariant mass and the dimuon invariant mass, and require $|(m_{\mu\mu h} - m_B) - (m_{\mu\mu} - m_{J/\psi^{(\prime)}})| > 100 \text{ MeV}/c^2$. $B \rightarrow J/\psi^{(\prime)}h$ decays with one hadron misidentified as a muon form a potential background to the rare decay search. We reject this class of background by requiring that all combinations of tracks of the candidate have an invariant mass that differs by at least $40 \text{ MeV}/c^2$ from the $J/\psi^{(\prime)}$ mass. We also reject candidates with track pairs with a mass within $\pm 25 \text{ MeV}/c^2$ of the $D^0 \rightarrow K^-\pi^+$ decay, or track triplets compatible with a mass within $\pm 25 \text{ MeV}/c^2$ of the $D^+ \rightarrow K^-\pi^+\pi^+$ or $D_s^+ \rightarrow K^+K^-\pi^+$ decays.

We further improve the signal to background ratio by an optimization of the selection based on discriminating variables. For this purpose, Monte Carlo (MC) simulations of the signal processes are used. We generate single b hadrons using the transverse momentum spectrum from $B \rightarrow J/\psi X$, measured by CDF [18]. Decays of all b hadrons are simulated using EVTGEN [24], with lifetimes from Ref. [23], allowing for a decay width difference between the B_s^0 mass eigenstates, $\Delta\Gamma/\Gamma = 0.12 \pm 0.06$ [25]. The decays $B^0 \rightarrow J/\psi K^{*0}$ and $B_s^0 \rightarrow J/\psi\phi$ are simulated according to the polarization amplitudes measured by CDF [26]. The dynamics of the rare decay processes are simulated according to the calculations of Ali *et al.* [11]. For $B_s^0 \rightarrow \mu^+\mu^-\phi$, we assume a mixture of 50% CP-even and 50% CP-odd states. The interactions of final state particles are simulated using a GEANT [27] model of the CDF II detector, digitized into the CDF event format, and reconstructed using the same software as in the processing of collision data. The detector simulation includes a full emulation of the CDF trigger system. We find that the transverse momentum spectrum of the B mesons of this measurement are on average higher than in the simulation. This can be explained by the presence of a B baryon component with low transverse momentum in the measurement used as input spectrum of the simulation [18]. To correct for this, the simulated events are weighted by a polynomial function, which is obtained from the ratio of data to MC transverse momentum distribution of the B meson.

We tighten the candidate selection to obtain the smallest expected statistical uncertainty on the measurement of the $B \rightarrow \mu^+\mu^-h$ branching ratios by finding the selection with the largest value of $N_{sig}/\sqrt{N_{sig} + N_{bkg}}$. The expected number of signal events, N_{sig} , is determined by scaling the MC yields of the rare decay modes to the yields of the normalization channels in the data, and correcting by the relative branching ratios and selection efficiencies. This procedure requires estimates of

the branching ratios of the rare decay modes. For the $B^+ \rightarrow \mu^+\mu^-K^+$ and $B^0 \rightarrow \mu^+\mu^-K^{*0}$ decays we use the world average measured branching ratios [23], while for $B_s^0 \rightarrow \mu^+\mu^-\phi$ we use the theoretical estimate [15]. The expected number of background events, N_{bkg} , is estimated by extrapolating the candidate yield with an invariant mass $(180 - 300) \text{ MeV}/c^2$ higher than the B mass, to the signal region. Candidates with an invariant mass lower than the B mass are not suitable for background estimates, since they contain partially reconstructed B decays, not expected in the signal region. We find good discriminating power between signal and background from the following three quantities: t/σ_t , α , and I . The significance of the proper decay time, t/σ_t , is defined as the proper decay time of the B candidate, divided by its uncertainty. The angle α is defined as the difference in angle between the B candidate's momentum vector and the vector from the primary vertex to the $\mu\mu h$ vertex. The isolation, I , is defined as the transverse momentum carried by the B meson candidate divided by the transverse momentum of all tracks in a cone of $\Delta R = \sqrt{\Delta\eta^2 + \Delta\phi^2} = 1.0$ around the direction of the B meson candidate, including those of the B candidate itself. Here $\Delta\eta$ is the difference in pseudorapidity of the B candidate and each track, and $\Delta\phi$ is the difference in their azimuthal angles. Scanning different combinations of selection thresholds, we find that the optimal values are very similar for the three rare decay modes: $t/\sigma_t \geq 14$, $\alpha \leq 60 \text{ mrad}$, and $I \geq 0.6$. Applying the optimized selection requirements to the normalization channels yields the distributions shown in Fig. 1. The shape of the combinatoric background is estimated from a sample with poor vertex quality (χ^2 probability $< 10^{-3}$). The invariant mass distribution of this poor vertex quality sample is fitted with a Gaussian distribution for the remaining signal contribution and an exponential plus a constant to model the background. We estimate the background in the signal region of the tight selection using this functional form, normalized to the number of candidates with invariant mass $(60 - 180) \text{ MeV}/c^2$ higher than the B mass. Using this method, we find $6361 \pm 82 B^+ \rightarrow J/\psi K^+$, $2423 \pm 52 B^0 \rightarrow J/\psi K^{*0}$, and $431 \pm 22 B_s^0 \rightarrow J/\psi\phi$ decays. The invariant mass distributions for the rare decay modes are shown in Fig. 2. In the $\pm 40 \text{ MeV}/c^2$ window around the B mass we find 90 $B^+ \rightarrow \mu^+\mu^-K^+$, 35 $B^0 \rightarrow \mu^+\mu^-K^{*0}$, and 11 $B_s^0 \rightarrow \mu^+\mu^-\phi$ candidates. From simulation studies we verified that the present selection accepts decays for every kinematically possible dimuon invariant mass, with an efficiency difference not exceeding a factor two, except for the windows around the $J/\psi^{(\prime)}$ that have been explicitly excluded.

For the signal modes, we evaluate three sources of background: the combinatoric background, hadrons misidentified as muons, and hadrons with misassigned mass. As in the normalization mode, the shape of the combinatoric background is estimated from a sample with poor vertex quality (χ^2 probability $< 10^{-3}$). The

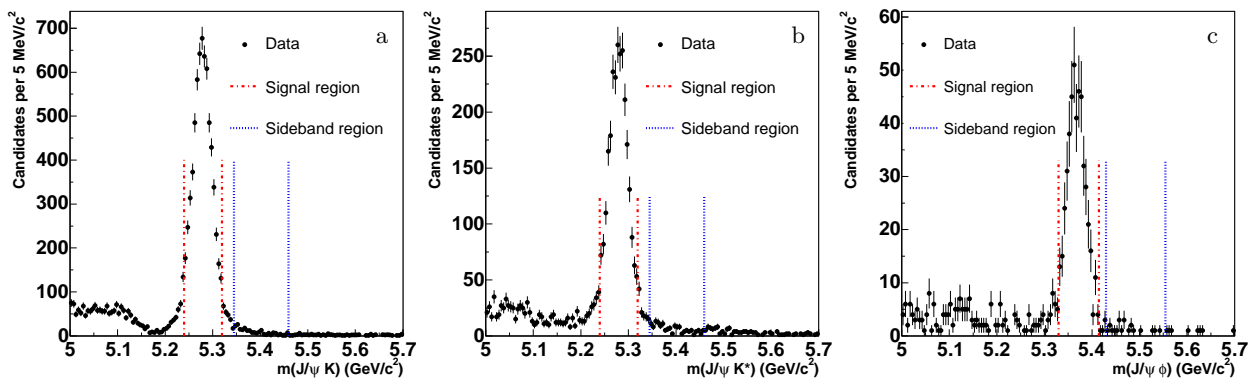


FIG. 1: Invariant mass spectra of (a) $J/\psi K^+$, (b) $J/\psi K^{*0}$ and (c) $J/\psi \phi$ candidates after applying optimized selection requirements.

invariant mass distribution of these candidates is fitted to an exponential plus a constant. This functional form is used to extrapolate the number of candidates with invariant mass ($60 - 180$) MeV/c^2 higher than the B mass to the signal region. The resulting backgrounds, and their statistical uncertainties, consist of 44.3 ± 5.8 , 16.3 ± 3.6 , and 3.1 ± 1.5 candidates for the $B^+ \rightarrow \mu^+ \mu^- K^+$, $B^0 \rightarrow \mu^+ \mu^- K^{*0}$, and $B_s^0 \rightarrow \mu^+ \mu^- \phi$ decay modes, respectively. Backgrounds from hadrons misidentified as muons are estimated from simulation. Final state particles from simulated charmless B decays are weighted with the muon misidentification probabilities. The misidentification probabilities for charged kaons and pions are measured from a sample of $D^{*+} \rightarrow D^0 \pi^+$ followed by $D^0 \rightarrow K^- \pi^+$ decays. We estimate a net background of 1.0 events for the $B^+ \rightarrow \mu^+ \mu^- K^+$ channel, primarily coming from misidentified $B^+ \rightarrow K^+ \pi^- \pi^+$ decays. For the B^0 and B_s^0 modes, this background is negligible. From simulation we determine the background contribution that arises from assigning the wrong masses to the hadrons. We estimate $0.4 B^0 \rightarrow \mu^+ \mu^- K^{*0}$ decays which are reconstructed as $B_s^0 \rightarrow \mu^+ \mu^- \phi$ and $0.2 B_s^0 \rightarrow \mu^+ \mu^- \phi$ decays reconstructed as $B^0 \rightarrow \mu^+ \mu^- K^{*0}$.

We calculate the signal yield by subtracting the predicted background from the number of candidates in the signal window. We find an excess in the B signal region in all three channels, and determine the significance by calculating the Poisson probability for the background to fluctuate to the number of observed events or higher, taking into account the uncertainty on the background. We find an equivalent Gaussian significance of 4.5, 2.9, and 2.4 standard deviations, respectively for the B^+ , B^0 , and B_s^0 modes.

Table I lists the systematic uncertainties associated with the relative selection efficiency, discussed in further detail below. To take into account the uncertainty on the relative efficiency due to uncertainties in the dynamics of the rare decays, we apply the weak form factors from Ref. [28, 29] and evaluate the largest difference between the reconstruction efficiency and the cen-

tral value. We find an uncertainty of 3.1% or less. The uncertainty related to the $p_T(B)$ spectrum is evaluated from the change in relative efficiency when the three parameters in the $p_T(B)$ weighting function are varied by one standard deviation of their values determined from fits to data, taking into account correlations. The difference reaches 1.4% in the B_s^0 mode. The muon trigger efficiency close to the $1.5 \text{ GeV}/c$ p_T threshold is poorly known. We find a change in the relative efficiency reaching 1.3% if the minimum p_T is varied by $\pm 100 \text{ MeV}/c$, covering the range over which the trigger efficiency rises from zero to one. The final state particles of the rare decay modes have approximately 10% more low momentum tracks than those of the normalization channels. The simulation models the track reconstruction efficiency to an accuracy of 2% in the p_T range of $0.4 - 1.5 \text{ GeV}/c$. We therefore assign a systematic uncertainty on the relative efficiency of $2\% \times 10\% = 0.2\%$. We find an uncertainty of 8.3% on the relative efficiency of B_s^0 decays due to the unknown fraction of the short-lived CP-even state in the rare decay mode. We assume that the CP-even fraction is 0.5, and assess systematic uncertainties for the extremes of the fraction valued at 1.0 and 0.0. In addition, the uncertainty on $\Delta\Gamma/\Gamma$ contributes another 2.6%, resulting in a total uncertainty of 8.7% associated with the B_s^0 decay width difference. This is the largest systematic uncertainty on the relative efficiency of the B_s^0 mode. We evaluate the effect of the uncertainty on the fraction of J/ψ mesons produced with a longitudinal polarization by varying the fraction measured at CDF [26] by $\pm 1\sigma$. The effect is 0.6% for $B^0 \rightarrow J/\psi K^{*0}$ and 0.1% for $B_s^0 \rightarrow J/\psi \phi$.

The statistical uncertainties of yields in the normalization channels are included as systematic uncertainties, which range from 1.3% for the B^+ channel to 5.1% for the B_s^0 channel. Cabibbo-suppressed $B^+ \rightarrow J/\psi \pi^+$ decays contribute 0.1% to the yield of the normalization channel for the B^+ channel. We introduce the full effect into our estimate of the systematic uncertainty without correcting the result. The relative efficiencies between signal

TABLE I: Systematic uncertainties on the relative efficiency quoted in percent.

Channel	B^+	B^0	B_s
Theory model	1.5	3.1	1.6
$p_T(B)$ spectrum	0.6	1.3	1.4
Trigger turn-on	1.3	1.3	1.2
Low momentum hadrons	0.2	0.2	0.2
B_s^0 decay width difference	–	–	8.7
Polarization	–	0.6	0.1
Norm. channel statistics	1.3	2.1	5.1
$B^+ \rightarrow J/\psi\pi^+$ contribution	0.1	–	–
MC statistics	1.6	2.6	2.2
Total	2.9	5.0	10.6

TABLE II: Summary of systematic uncertainties quoted in percent.

Channel	B^+	B^0	B_s
Total rel. eff. uncertainty	2.9	5.0	10.6
$\mathcal{B}(J/\psi \rightarrow \mu^+\mu^-)$	1.0	1.0	1.0
Background prediction	5.2	3.1	10.2
$\mathcal{B}(B \rightarrow J/\psi h)$	3.5	4.5	35.5

and normalization channels, of 0.71 ± 0.01 , 0.74 ± 0.02 , and 0.84 ± 0.02 for the B^+ , B^0 , and B_s^0 decays, respectively, have uncertainties reaching 2.6%, that arise from the finite size of the MC samples.

The predicted background values depend on the shape of the background function. We evaluate the change in the background yield calculation when using a sample that is similar to the one resulting from the optimal selection, but has less stringent requirements on the three optimization variables instead of the default sample with poor vertex quality. We compare two functional models for the background description, the default exponential plus a constant, and a simpler linear extrapolation function. We find a systematic uncertainty on the background prediction reaching 10% for the B_s^0 channel.

To calculate the systematic uncertainty on the relative branching fraction, the relative efficiency uncertainty is summed in quadrature with the uncertainty of the $J/\psi \rightarrow \mu^+\mu^-$ branching ratio, and with the systematic uncertainty on the number of signal candidates.

To calculate the absolute branching fractions, we use the world average branching fractions of the normalization channels [23]. These branching fractions have uncertainties of 3.5%, 4.5%, and 35.5%, respectively, for B^+ , B^0 , and B_s^0 , which are added in quadrature to the systematic uncertainties on the relative branching ratios. A summary of the systematic uncertainties is given in Table II.

We calculate relative branching ratios using Eq. (1), and find $\mathcal{B}(B^+ \rightarrow \mu^+\mu^-K^+)/\mathcal{B}(B^+ \rightarrow J/\psi K^+) = (0.59 \pm 0.15 \pm 0.03) \times 10^{-3}$, $\mathcal{B}(B^0 \rightarrow \mu^+\mu^-K^{*0})/\mathcal{B}(B^0 \rightarrow$

$J/\psi K^{*0}) = (0.61 \pm 0.23 \pm 0.07) \times 10^{-3}$, and $\mathcal{B}(B_s^0 \rightarrow \mu^+\mu^-\phi)/\mathcal{B}(B_s^0 \rightarrow J/\psi\phi) = (1.23 \pm 0.60 \pm 0.14) \times 10^{-3}$, where the first uncertainty is statistical, and the second is systematic. We use the world-average branching ratios of the B^0 and B^+ normalization channels [23], resulting in the following absolute branching fractions: $\mathcal{B}(B^+ \rightarrow \mu^+\mu^-K^+) = (0.59 \pm 0.15 \pm 0.04) \times 10^{-6}$, and $\mathcal{B}(B^0 \rightarrow \mu^+\mu^-K^{*0}) = (0.81 \pm 0.30 \pm 0.10) \times 10^{-6}$. To obtain an absolute branching ratio for the $B_s^0 \rightarrow \mu^+\mu^-\phi$ decay, we use $\mathcal{B}(B_s^0 \rightarrow J/\psi\phi) = (1.38 \pm 0.49) \times 10^{-3}$, obtained from correcting the CDF measurement [30] for the current value of f_s/f_d [23], the B_s^0 to B^0 production ratio, resulting in $\mathcal{B}(B_s^0 \rightarrow \mu^+\mu^-\phi) = (1.70 \pm 0.82 \pm 0.64) \times 10^{-6}$. We find a significance of only 2.4 standard deviations for the $B_s^0 \rightarrow \mu^+\mu^-\phi$ decay mode. Therefore, we choose to set a limit on this decay. We use a Bayesian integration assuming a flat prior [31], and find $\mathcal{B}(B_s^0 \rightarrow \mu^+\mu^-\phi)/\mathcal{B}(B_s^0 \rightarrow J/\psi\phi) < 2.6(2.3) \times 10^{-3}$ at the 95(90)% confidence level (C.L.). We also set an upper limit on the absolute branching ratio, taking into account the uncertainty of the branching ratio of the normalization channel [32]. We assume that the prior probability density function representing the uncertainty in the normalization channel is a log normal distribution with a mean equal to the central value, and a width parameter equal to the quoted uncertainty of 35.5%. We obtain $\mathcal{B}(B_s^0 \rightarrow \mu^+\mu^-\phi) < 6.0(5.0) \times 10^{-6}$ at 95(90)% C.L. The main ingredients and the results are summarized in Table III.

In conclusion, our measurements of the B^+ and B^0 rare decay modes are consistent with the SM predictions, and with previous measurements [5, 6]. The relative limit on $B_s^0 \rightarrow \mu^+\mu^-\phi$ is consistent with the SM predictions, and is the most stringent to date.

Acknowledgments

We thank the Fermilab staff and the technical staffs of the participating institutions for their vital contributions. This work was supported by the U.S. Department of Energy and National Science Foundation; the Italian Istituto Nazionale di Fisica Nucleare; the Ministry of Education, Culture, Sports, Science and Technology of Japan; the Natural Sciences and Engineering Research Council of Canada; the National Science Council of the Republic of China; the Swiss National Science Foundation; the A.P. Sloan Foundation; the Bundesministerium für Bildung und Forschung, Germany; the Korean Science and Engineering Foundation and the Korean Research Foundation; the Science and Technology Facilities Council and the Royal Society, UK; the Institut National de Physique Nucleaire et Physique des Particules/CNRS; the Russian Foundation for Basic Research; the Comisión Interministerial de Ciencia y Tecnología, Spain; the European Community's Human Potential Programme; the Slovak R&D Agency; and the Academy of Finland.

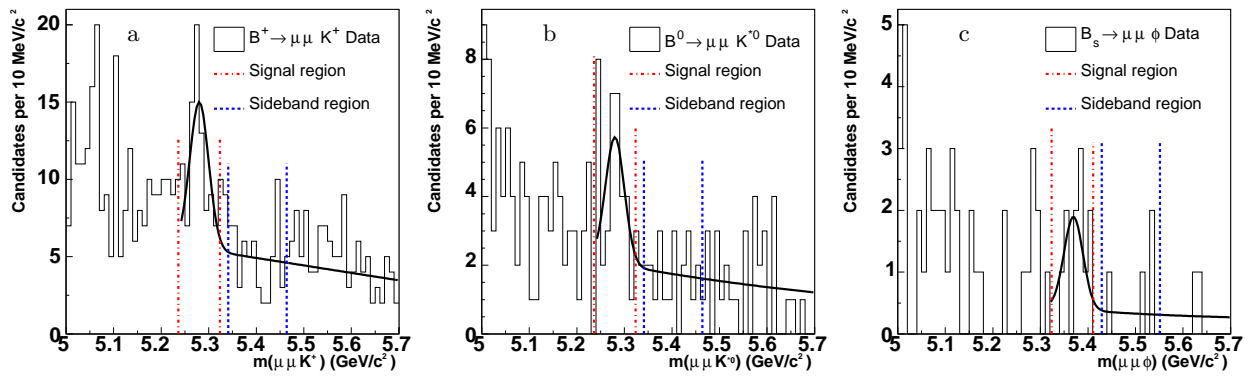


FIG. 2: Invariant mass spectra of (a) $\mu^+\mu^-K^+$, (b) $\mu^+\mu^-K^{*0}$ and (c) $\mu^+\mu^-\phi$ candidates. The superimposed curves are a sum of a single Gaussian with a width of $20 \text{ MeV}/c^2$ representing the signal, and a curve representing the background as determined by the procedure described in the text. The curves are not drawn for masses below the signal window, since they are not expected to predict the background level where partially reconstructed B decays contribute.

TABLE III: Summary of the main ingredients and results of this analysis. Where one uncertainty is quoted, the uncertainty is of statistical nature. Where two uncertainties are quoted, the first is statistical, and the second is systematic.

Decay mode	$B^+ \rightarrow \mu^+\mu^-K^+$	$B^0 \rightarrow \mu^+\mu^-K^{*0}$	$B_s^0 \rightarrow \mu^+\mu^-\phi$
N_{obs}	90	35	11
N_{bkg}	45.3 ± 5.8	16.5 ± 3.6	3.5 ± 1.5
N_{sig}	44.7 ± 5.8	18.5 ± 3.6	7.5 ± 1.5
Gaussian significance	4.5σ	2.9σ	2.4σ
$N_{J/\psi h}$	6361 ± 82	2423 ± 52	431 ± 22
$\epsilon_{\mu^+\mu^-h}/\epsilon_{J/\psi h}$	0.71 ± 0.01	0.74 ± 0.02	0.84 ± 0.02
Rel $\mathcal{B} \times 10^3$	$0.59 \pm 0.15 \pm 0.03$	$0.61 \pm 0.23 \pm 0.07$	$1.23 \pm 0.60 \pm 0.14$
Abs $\mathcal{B} \times 10^6$	$0.59 \pm 0.15 \pm 0.04$	$0.81 \pm 0.30 \pm 0.10$	$1.70 \pm 0.82 \pm 0.64$
Rel \mathcal{B} 95(90)%C.L. limit $\times 10^3$	—	—	2.6(2.3)
Abs \mathcal{B} 95(90)%C.L. limit $\times 10^6$	—	—	6.0(5.0)

- [1] P. Colangelo, F. De Fazio, R. Ferrandes, and T. N. Pham, Phys. Rev. D **73**, 115006 (2006).
- [2] F. Kruger and J. Matias, Phys. Rev. D **71**, 094009 (2005).
- [3] T. M. Aliev, A. Ozpineci, and M. Savci, Eur. Phys. J. C **29**, 265 (2003).
- [4] D. A. Demir, K. A. Olive, and M. B. Voloshin, Phys. Rev. D **66**, 034015 (2002).
- [5] B. Aubert *et al.* (BABAR Collaboration), Phys. Rev. D **73**, 092001 (2006).
- [6] A. Ishikawa *et al.* (Belle Collaboration), Phys. Rev. Lett. **91**, 261601 (2003).
- [7] G. Burdman, Phys. Rev. D **52**, 6400 (1995)
- [8] P. Colangelo, F. De Fazio, P. Santorelli, and E. Scrimieri, Phys. Rev. D **53**, 3672 (1996) [Erratum-ibid. D **57**, 3186 (1998)]
- [9] T. M. Aliev, A. Ozpineci, and M. Savci, Phys. Rev. D **56**, 4260 (1997)
- [10] D. Melikhov, N. Nikitin, and S. Simula, Phys. Rev. D **57**, 6814 (1998)
- [11] A. Ali, P. Ball, L. T. Handoko, and G. Hiller, Phys. Rev. D **61**, 074024 (2000).
- [12] H. M. Choi, C. R. Ji, and L. S. Kisslinger, Phys. Rev. D **65**, 074032 (2002)
- [13] A. Ali, E. Lunghi, C. Greub, and G. Hiller, Phys. Rev. D **66**, 034002 (2002)
- [14] C. H. Chen and C. Q. Geng, Phys. Rev. D **66**, 094018 (2002)
- [15] C. Q. Geng and C. C. Liu, J. Phys. G **29**, 1103 (2003).
- [16] V. M. Abazov *et al.* (D0 Collaboration), Phys. Rev. D **74**, 031107 (2006).
- [17] D. Acosta *et al.* (CDF Collaboration), Phys. Rev. D **65**, 111101 (2002).
- [18] D. Acosta *et al.* (CDF Collaboration), Phys. Rev. D **71**, 032001 (2005).
- [19] A. Sill *et al.*, Nucl. Instrum. Methods A **447**, 1 (2000).
- [20] A. A. Affolder *et al.*, Nucl. Instrum. Methods A **526**, 249 (2004).
- [21] G. Ascoli *et al.*, Nucl. Instrum. Methods A **268**, 33 (1988).
- [22] The CDF reference frame uses cylindrical coordinates, where θ and ϕ are the polar and azimuthal angles with respect to the proton beam. Pseudorapidity η is defined

- as $-\ln(\tan(\theta/2))$.
- [23] W.-M. Yao *et al.*, J. Phys. G **33**, 1 (2006).
 - [24] D. J. Lange, Nucl. Instrum. Methods A **462**, 152 (2001).
 - [25] I. Dunietz, R. Fleischer, and U. Nierste, Phys. Rev. D **63**, 114015 (2001).
 - [26] D. Acosta *et al.* (CDF Collaboration), Phys. Rev. Lett. **94**, 101803 (2005).
 - [27] R. Brun *et al.*, CERN Program Library Long Writeup W5013 (1994).
 - [28] D. Melikhov and B. Stech, Phys. Rev. D **62**, 014006 (2000).
 - [29] P. Colangelo, F. De Fazio, and P. Santorelli, Phys. Rev. D **51**, 2237 (1995).
 - [30] F. Abe *et al.*, (CDF Collaboration), Phys. Rev. D **54**, 6596 (1996).
 - [31] J. Heinrich, C. Blocker, J. Conway, L. Demortier, L. Lyons, G. Punzi, and P. K. Sinervo, arXiv:physics/0409129.
 - [32] Note that the uncertainty in the normalization mode's branching ratio was not taken into account in [16].